Copyright Warning & Restrictions

The copyright law of the United States (Title 17, United States Code) governs the making of photocopies or other reproductions of copyrighted material.

Under certain conditions specified in the law, libraries and archives are authorized to furnish a photocopy or other reproduction. One of these specified conditions is that the photocopy or reproduction is not to be "used for any purpose other than private study, scholarship, or research." If a, user makes a request for, or later uses, a photocopy or reproduction for purposes in excess of "fair use" that user may be liable for copyright infringement,

This institution reserves the right to refuse to accept a copying order if, in its judgment, fulfillment of the order would involve violation of copyright law.

Please Note: The author retains the copyright while the New Jersey Institute of Technology reserves the right to distribute this thesis or dissertation

Printing note: If you do not wish to print this page, then select "Pages from: first page # to: last page #" on the print dialog screen

NJIT New Jersey's Science & Technology University

The Van Houten library has removed some of the personal information and all signatures from the approval page and biographical sketches of theses and dissertations in order to protect the identity of NJIT graduates and faculty.

ABSTRACT

SINGLE-CARRIER FREQUENCY DOMAIN EQUALIZATION USING SUBBAND DECOMPOSITION FOR OPTICAL WIRELESS COMMUNICATIONS

by
Di Mu

Optical wireless communication is intended to be applied into indoor and visual distance high-rate data transmission, which is complementary to radio frequency communications. There are specific problems and requirements in optical wireless communications compared with radio frequency communications. Single-carrier frequency domain equalization (SCFDE) is a transmission scheme which has been considered as an alternative of orthogonal frequency-division multiplexing (OFDM), because it has most of the advantages of OFDM and avoids the problems of OFDM. Subband decomposition is a multi-resolution signal analysis and synthesis method, using quadrature mirror filter (QMF) bank to convert time-domain signal to frequency-domain subbands. As a time-to-frequency transform, subband decomposition technique can be employed to frequency domain equalization. Compared with the commonly used discrete Fourier transform (DFT), subband transform is more flexible and efficient to compensate the fading of frequency-selective channels.

This thesis includes the theories of SCFDE, subband decomposition, subband equalization, and optical wireless transmission scheme. Also, simulations are given to demonstrate the processing of signals and the implementation of equalizers. The results show that the transmitted signal can be effectively equalized to compensate the channel fading, and the transmission scheme is appropriate for optical wireless communications.

SINGLE-CARRIER FREQUENCY DOMAIN EQUALIZATION USING SUBBAND DECOMPOSITION FOR OPTICAL WIRELESS COMMUNICATIONS

by
Di Mu

A Master's Thesis
Submitted to the Faculty of
New Jersey Institute of Technology
in Partial Fulfillment of the Requirements for the Degree of
Master of Science in Electrical Engineering

Department of Electrical and Computer Engineering

January 2012

Copyright © 2011 by Di Mu

ALL RIGHTS RESERVED

.

APPROVAL PAGE

SINGLE-CARRIER FREQUENCY DOMAIN EQUALIZATION USING SUBBAND DECOMPOSITION FOR OPTICAL WIRELESS COMMUNICATIONS

Di Mu

Dr. Yeheskel Bar-Ness, Committee Member — Date
Distinguished Professor of Electrical and Computer Engineering, NJIT

Dr. Ali N Akansu, Committee Member — Date
Professor of Electrical and Computer Engineering, NJIT

Dr. Richard A Haddad, Committee Member — Date
Professor of Electrical and Computer Engineering, NJIT

BIOGRAPHICAL SKETCH

Author: Di Mu

Degree: Master of Science

Date: December 2011

Undergraduate and Graduate Education:

- Master of Science in Electrical Engineering,
  New Jersey Institute of Technology, Newark, NJ, 2011

- Bachelor of Science in Communication Engineering,
  Hangzhou Dianzi University, Zhejiang, P. R. China, 2010

Major: Electrical Engineering

道可道，非常道；名可名，非常名。

— 老子

A principle which can be told is not a permanent principle;
A name which can be given is not a permanent name.

— Laozi (604 BC - ?)

ACKNOWLEDGMENT

First of all, I would like to appreciate my thesis advisor, Dr. Yeheskel Bar-Ness for his support and encouragement. He introduced me to the novel technique of SC-FDE and advanced principles in wireless communications. His help is very important to my thesis work. Great thanks to him.

I also appreciate Dr. Ali N Akansu and Dr. Richard A Haddad for their teaching and help. Dr. Akansu, my co-advisor, introduced me to the multi-resolution signal decomposition technique, which has been applied into the thesis topic. Dr. Haddad is the instructor of my two fundamental courses, providing essential knowledge for further research. Thanks a lot to them.

Finally, it's the great thanks to my family – my father, my mother, my two grandmothers, my uncles, my aunts, and my cousins. With their care and love, I could complete the study oceans away from home.

TABLE OF CONTENTS

LIST OF FIGURES

CHAPTER 1

INTRODUCTION

1.1 Optical Wireless Communication

With the growing number of information devices used in work and at home, the need of indoor high-rate wireless transmission has been increasing. Due to the limitation of radio frequency (RF) spectrum, RF systems can only provide limited bandwidth to the end users. However, optical wireless communication is complementary and alternative to RF communication because of its unlimited optical spectrum. The restrictions of RF systems don't apply to optical wireless communication. Optical signal is more effective in a short distance than in a long distance, thus it's a good option for indoor communication.

In optical wireless communications, light emitting diodes (LEDs) are mostly used as transmitters, and photo-diodes are used as optical signal receivers. The block diagram of an optical wireless communication system is shown as Figure 1.1. The optoelectronic components like LEDs and photo-diodes are much cheaper than RF devices like antennas and amplifiers.

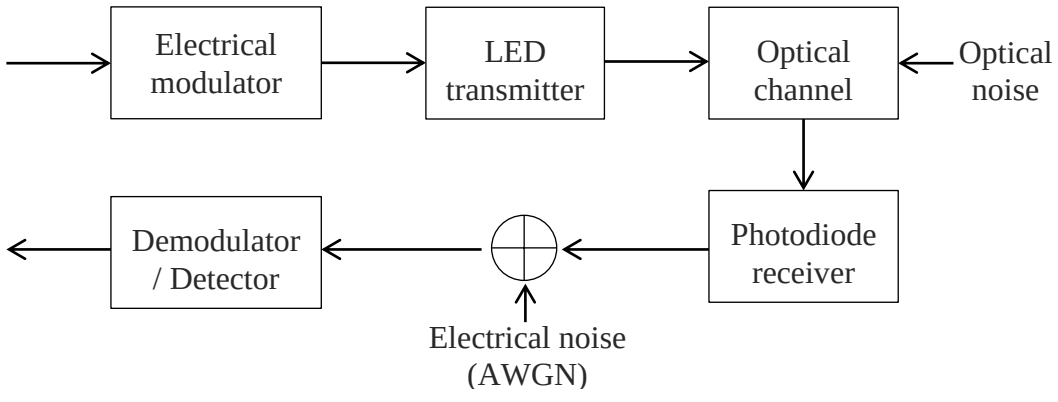

Figure 1.1 Block diagram of an optical wireless communication system [1].

Optical wireless communication has two special requirements as compared to RF wireless communication. **First,** the transmitted signal must be real and positive. Because the transmitted signal is represented by the voltage on the LEDs, the voltage must be real and positive to convert to optical signal. **Second,** the lower peak-to-average power ratio (PAPR) is preferred. LEDs only have a short linear range in I-V curve, so if the transmitted signal has high peaks in amplitude, the signal will be affected by the nonlinear behavior of LEDs.

Similar to RF channels, optical channels also might be multi-path, due to the reflections from walls and objects. Multi-path propagation often brings inter-symbol interference (ISI) at the receiver, resulting in bit errors. Equalization is a typical method to combat ISI and recover the symbols. Generally, the transmission method of an optical wireless communication system is intended to provide a low PAPR and an effective equalizer.

1.2 Transmission Methods

In the field of digital communications, a transmission method typically includes modulation/ demodulation, channel coding/ decoding, and equalization. The design of a transmission method is so important that it determines the service quality of a communication system.

Recently two sorts of transmission schemes have been researched to provide effective equalization processes, which are multi-carrier transmission and single-carrier transmission. Multi-carrier transmission schemes, such as discrete multi-tone (DMT) and orthogonal frequency division multiplexing (OFDM), equalize the signal by using a number of subcarriers into the whole bandwidth, and adjusting the amplitude of each

subcarrier. Single-carrier transmission, such as single-carrier frequency domain equalization (SCFDE), has only one carrier frequency, and equalizes the signal by a processing in frequency domain.

Orthogonal frequency division multiplexing (OFDM) has been considered as a transmission scheme for optical wireless communication. It offers the advantages to combat inter-symbol interference (ISI) caused by multi-path channels. The equalization of OFDM signals is in time domain, called time domain equalization (TDE). OFDM can also provide high data rate and high bandwidth efficiency. Due to these advantages, it has been applied to digital subscriber line (DSL) connections and mobile downlink transmissions. Despite to its contributions, OFDM signals have inherently high PAPR, which limits its application in optical wireless communication. A high PAPR may cause the distortion of the received signal and the decrement of signal resolution. In fact, high PAPR is a common property of most multi-carrier transmission schemes (including OFDM). Single-carrier signals, on the other hand, provide much lower PAPR than multi-carrier signals. Thus, naturally we have more interest in single-carrier transmission as an alternative of OFDM for optical wireless communication. Single-carrier frequency domain equalization (SCFDE) is a typical single-carrier transmission scheme and to be discussed in further chapters.

Generally, in this thesis, the transmission method to be discussed is designed for high-rate optical wireless communication with indoor or visual distance environments. It will be explained that SCFDE is a suitable method for this application. An important part of SCFDE we tackle in this thesis is the use of equalization which is implemented by the quadrature mirror filter (QMF) bank that based on Daubechies filters.

CHAPTER 2

SCFDE FOR OPTICAL WIRELESS COMMUNICATION

2.1 Transmission Scheme

Single-carrier frequency domain equalization (SCFDE) is a transmission method that supports effective equalization and provides low transmitted peak-to-average power ratio (PAPR). The block diagram of SCFDE is similar to OFDM in most of the parts, but the transmitted signal spectrum is entirely changed by adding two blocks of transform processes. Also, equalization is changed to frequency domain from OFDM scheme.

As the block diagram (Figure 2.1) shows, data symbols are modulated by QPSK (quadrature phase shift keying) or QAM (quadrature amplitude modulation). Then, the modulated sequence is transformed to frequency domain, by a specifically designated transform method. Traditionally, FFT (fast Fourier transform) is the transform method used in OFDM. As an alternative to OFDM, a new technique of QMF is discussed in the next chapter. The transformed signal in frequency domain is coded in order to compensate for the selective frequency fading of channels. Then inverse transform is used to convert frequency domain signal back to time domain. After adjusting the voltage of the transmitted signal, this signal is output to LED(s).

The transmitted optical signal goes through the optical channel which might be multi-path, and is received by photodiode(s). As an inverse process of the transmitter, the received signal is transformed to frequency domain, and gets equalized to compensate channel affects. Finally the equalized received signal is recovered back to time domain and demodulated by a symbol detector.

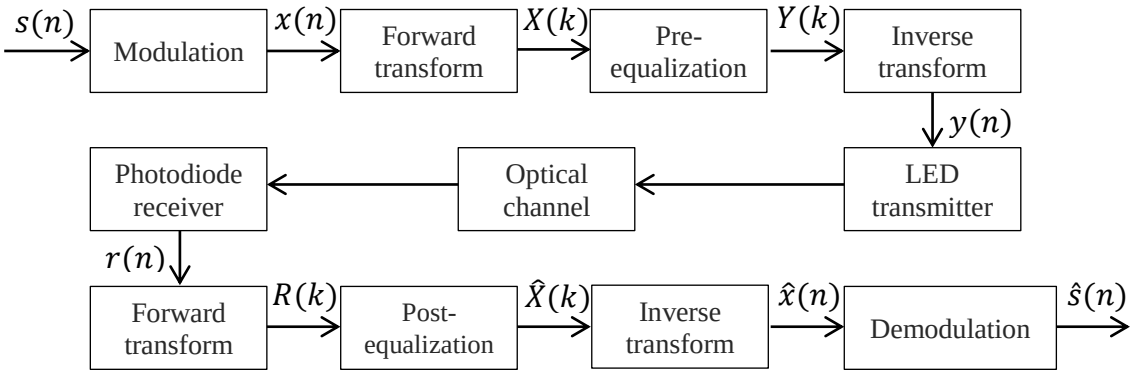

Figure 2.1 Block diagram of a basic SCFDE transmission scheme.

2.2 PAPR Analysis

In this section, the peak-to-average power ratio (PAPR) performances of multi-carrier and single-carrier signals are compared. To begin with, we will explain the features of multi-carrier and single-carrier signals, and find the most important difference. Figure 2.2 shows examples of the spectrums of these two kinds of signals.

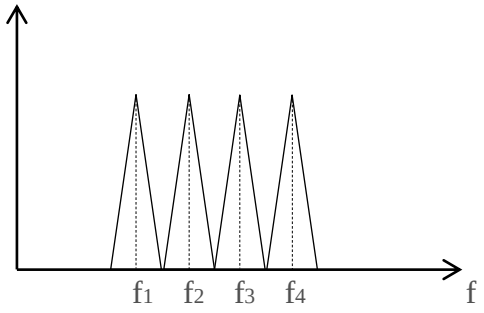

Figure 2.2(a) Multi-carrier spectrum.

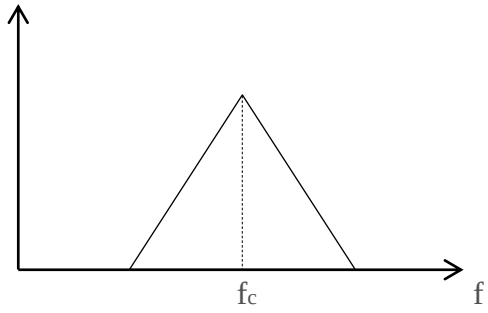

Figure 2.2(b) Single-carrier spectrum.

As shown above, multi-carrier signals have multiple subcarriers. Each subcarrier has its center frequency and identical bandwidth. Subcarriers can be clearly separated by a same frequency difference. On the other hand, single-carrier signals have only one carrier with one center frequency. The entire bandwidth cannot be separated to more than one part.

The PAPR performance can be analyzed in these two schemes. PAPR of the transmitted signal is defined by

$$PAPR\{y(n)\} = \frac{\max\{|y(n)|^2\}}{E\{|y(n)|^2\}}, \tag{2.1}$$

where E{ • } is the statistical average operator. As its name, PAPR is the ratio of the peak power to average power.

Define a multi-carrier signal $m(t)$ as the sum of cosine waves with variant frequencies in Equation (2.2),

$$\begin{aligned} m(t) &= \cos(\omega_c - (M/2)\cdot\omega_d)t + \cos(\omega_c - (M/2+1)\cdot\omega_d)t + \cdots + \cos(\omega_c t) + \cdots \\ &\quad + \cos(\omega_c + (M/2-1)\cdot\omega_d)t \\ &= \sum_{i=-M/2}^{M/2-1} \cos(\omega_c + i\cdot\omega_d)t\,, \end{aligned} \tag{2.2}$$

where ω_c is the central frequency, ω_d is the frequency difference between each subcarrier, and M is an even integer which is the number of subcarriers.

To find the maximum value of $|m(t)|^2$, just take square of the maximum value of $|m(t)|$. In other words, the peak power equals the square of the peak amplitude.

$$\max\{|m(t)|^2\} = \{\max(|m(t)|)\}^2 \tag{2.3}$$

$m(t)$ gets the peak amplitude when all cosine components get the peak. Because cosine is periodic function, no matter what are the values of M and ω_d, there must exist a $\boldsymbol{t}$ satisfying all of the following equations,

$$\begin{aligned} (\omega_c - (M/2)\cdot\omega_d)t &= N_1\cdot 2\pi \\ (\omega_c - (M/2+1)\cdot\omega_d)t &= N_2\cdot 2\pi \\ &\cdots\cdots \\ (\omega_c + (M/2-1)\cdot\omega_d)t &= N_M\cdot 2\pi\,, \end{aligned} \tag{2.4}$$

where $N_1, N_2, \ldots, N_M$ are integers. In this condition of t, all of the cosine components get their peak value – 1. And thus, $m(t)$ which is the sum the M cosine components will get the peak amplitude – M. So the peak power concluded for a M-subcarrier cosine signal is

$$\max\{|m(t)|^2\} = \{\max(|m(t)|)\}^2 = M^2 \ . \tag{2.5}$$

Now, the average power of $m(t)$ which equals $E\{|m(t)|^2\}$ is going to be discussed. Because each cosine component with different frequency is uncorrelated to other cosine components, namely

$$R_{m,n} = E\{\cos(\omega_c + m \cdot \omega_d)\, t \cdot \cos(\omega_c + n \cdot \omega_d)t\} = 0, \tag{2.6}$$

where m and n are any integers. Then, the average power equals the sum of the power of these cosine components, namely

$$E\{|m(t)|^2\} = \sum_{i=-M/2}^{M/2-1} E\{\cos^2(\omega_c + i \cdot \omega_d)\, t\} = M/2 \ . \tag{2.7}$$

Therefore, the PAPR of the multi-carrier signal is proportional to the number of subcarriers M, because

$$PAPR\{m(t)\} = \frac{\max\{|m(t)|^2\}}{E\{|m(t)|^2\}} = \frac{M^2}{M/2} = 2M \sim M \ . \tag{2.8}$$

Conclusively, PAPR will get larger with the increment of the number of subcarriers. If the number of subcarrier is one, or it is a single-carrier signal, the PAPR is lower than any multi-carrier signal. Therefore, single-carrier transmission is a better choice to be implemented in optical wireless communication system which requires lower PAPR.

2.3 Multipath Channel Analysis

Optical channels are very likely to be multipath, especially with indoor environment. Comparing to RF signals, optical signals are inherently having quite shorter wavelength (less than one micro-meter), and thus diffraction can hardly happen in optical transmissions. The most happening phenomenon of optical signals is reflection. The reflections of optical signals result in a multipath channel from transmitter to receiver. In an indoor environment, all of walls, ground, and objects can reflect optical signals. The photodiode may receive a number of echoes from these reflections, and the mixed echoes result in "time dispersion", which means the duration of the received symbols is greater than the transmitted symbols. Inter-symbol interference (ISI) may occur when "time dispersion" presents. Furthermore, multipath channels, which are similar to filters, may cause different attenuation to different frequency signals or signal components, which is called "frequency selective fading".

Due to these multi-path effects like "time dispersion" and "frequency selective fading", the transmitted signal can be distorted through the transmission, and the maximum bandwidth of the transmitted signal is limited by multipath channels. There is an approximate calculation of maximum transmitted bandwidth through multipath channels, in the following description.

Define "maximum excess delay" (τ_m) as the actual delay minus the delay of the first path [9],

$$\tau_m = \tau_x - \tau_1 \tag{2.9}$$

where τ_1 is the delay of the first echo, τ_x is the actual delay which equals to the delay of the last significant echo. In the absence of equalization, the approximate maximum transmission bandwidth of the channel is given by

$$B_{max} = k \cdot \frac{1}{\tau_m} \tag{2.10}$$

where k is a constant depending on the channel, but customarily is taken to be $1/4$ [9]. Assuming the transmission environment is a large room like a meeting hall, the distances travelled by multipath echoes can be very different due to reflections. Assume that the largest difference of the echo travelled distances is d_m and equals 30 meters, so maximum excess delay τ_m is given by

$$\tau_m = \frac{d_m}{C} = \frac{30}{3 \cdot 10^8} = 10^{-7}\ sec \tag{2.11}$$

where C is the speed of light. Thus, in the absence of equalizers, the approximate maximum transmission bandwidth of the channel is

$$B_{max} = k \cdot \frac{1}{\tau_m} = \frac{0.25}{10^{-7}} = 2.5\ MHz\ . \tag{2.12}$$

That means if the bandwidth of the transmitted signal is less than $2.5\ MHz$, there will be no significant distortion or frequency selective fading. But if the bandwidth is greater than $2.5\ MHz$, the transmitted signal will be heavily distorted by multipath effects. For many applications that require high-rate data transmission, this bandwidth limit is not acceptable. For the need of larger bandwidth, equalizers are used to compensate frequency selective fading. Therefore, with the presence of equalization, the transmitted signal can be recovered while the transmitted bandwidth is greater than the bandwidth limit of the channel.

2.4 Frequency Domain Equalization

The equalizers are used as two ways in SCFDE transmission scheme – "pre-equalization" in the transmitter and "post-equalization" in the receiver (see Figure 2.1). Both of them employ frequency domain equalization (FDE) scheme and use the same algorithm to compensate channel distortion. The only difference of them is that "pre-equalization" happens before the signal transmitted, but "post-equalization" occurs after the signal is received. As the actual requirement of application, one of them could be removed, or both of them could work together. For example, the "post-equalizer" could be removed if the transmitter knows the channel frequency response. Then, only the "pre-equalizer" in the transmitter works to compensate the channel distortion, and the receiver can save the computational cost because of no equalizer in the receiver.

If the transmitter doesn't know the channel exactly, the pre-equalizer can still roughly put a gain to the higher frequency components and enlarge them, because they are more likely to be attenuated. Furthermore, frequency selective channels might have a large attenuation in a certain range of frequency. The transmitted signal will be heavily distorted and can hardly get recovered in this frequency. Thus, if the pre-equalizer puts a gain to a frequency range which covers the large attenuation frequency, the post-equalizer can be more likely to recover the signal to the original one. Any change to spectrum by the channel and the pre-equalizer is supposed to be cancelled by the post-equalizer.

Basically, frequency domain equalization takes three steps as shown in Figure 2.2. **First**, the original signal passes through a forward transform and decomposed into frequency components. **Second**, the frequency domain signal is multiplied by a set of coefficients, which are designed to compensate the frequency selective fading of the

channel. **Third**, the equalized frequency domain signal passes through an inverse transform to convert back to time domain.

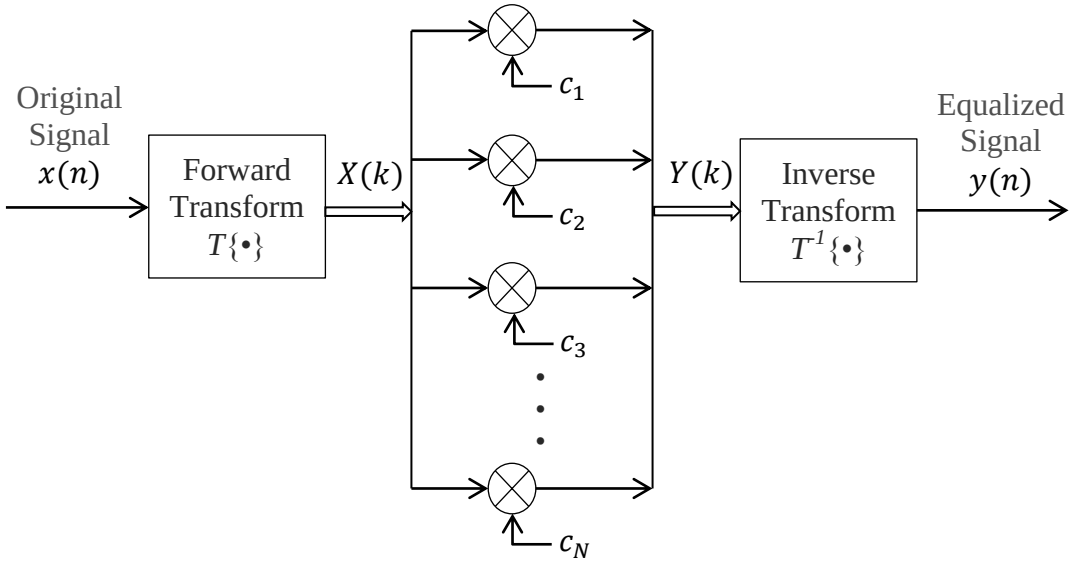

Figure 2.2 Basic frequency domain equalization scheme.

Define the forward transform operator $T\{\cdot\}$ and inverse transform operator $T^{-1}\{\cdot\}$, which give

$$X(k) = T\{x(n)\}, and\ \ x(n) = T^{-1}\{X(k)\}. \tag{2.13}$$

$c_1, c_2, \dots, c_N$ are a set of equalization coefficients in frequency domain, and are designed in different ways. The frequency-domain equalized signal $Y(k)$ is gotten by multiplying $X(k)$ and c_k. Therefore, the length of c_k has to be the same as the transform size. By the inverse transform of $Y(k)$, finally the equalized signal $y(n)$ is reconstructed into time domain.

The coefficients $c_1, c_2, \dots, c_N$ can be designed in different ways for different purposes. As one of the commonly used methods, the coefficients can satisfy the "zero-forcing" criterion of linear equalization [7], as the following equation

$$c_k = H(f)^{-1}|_{f=f_0 \cdot k}, \tag{2.14}$$

where $H(f)$ is the channel frequency response in continuous frequency, and f_0 is the minimum frequency resolution of the equalizer. Zero-forcing criterion is effective when ISI is more considerable than noise.

The flexibility of frequency analysis resolution is preferred in many applications. If the coefficients are used in the pre-equalizer in transmitters, sometimes they are just designed to roughly enlarge some frequency components which might be deeply attenuated through the channel. In this way, it is no need to have a very fine frequency resolution, but a rough resolution is acceptable. For example, assume the coherent bandwidth of a channel is B_c, and the transmitted signal bandwidth is B_X which is greater than B_c. The higher frequency components are enlarged by the pre-equalizer, and the lower frequency components remain as they are. So the coefficients $c_1, c_2, \dots, c_N$ are designed in the following equation,

$$c_k = \begin{cases} 1 & ,f_0 \cdot k < B_c \\ A & ,f_0 \cdot k > B_c \end{cases} \tag{2.15}$$

where *A* is the gain to the higher frequency components.

One can notice from Equation (2.15) that it is not necessary to have many transformed frequency points. In other words, it is better if the signal could be decomposed to just two subbands – one is for frequency less than B_c, the other one is for frequency larger than B_c – and map these subbands with only two coefficients. But in other applications, more coefficients with finer frequency resolution might be required to finely compensate the channel fading. Therefore, a flexible method that supports variant frequency resolutions is preferred for signal analysis and equalization. This is a sort of idea of "multi-resolution signal decomposition", which is discussed in the next chapter as an improvement of general transform methods. General transform methods, like Discrete

Fourier Transform (DFT), are the kind of “constant frequency resolution” transforms, which take fixed frequency steps. This fixed resolution model is employed in the previous discussions because it is a basic form of frequency domain equalization. In the next chapter, the multi-resolution transform method is applied to equalization.

CHAPTER 3

SUBBAND-BASED SCFDE

3.1 Daubechies Wavelet Filters

Daubechies Wavelets are a set of orthogonal wavelets that support multi-resolution analysis. They provide us powerful scaling functions (or father wavelet) and wavelet functions (or mother wavelet) to generate quadrature mirror filter (QMF) banks. These wavelets are originally designed for discrete wavelet transform (DWT) method. But in this chapter, the wavelet coefficients are employed to implement a QMF bank which is equivalent to the wavelet approach. These QMF filters are named "Binomial QMF", which are proved to be identical to Daubechies wavelet filters in Reference [14]. QMF is a method of subband decomposition technique, which uses a set of filters to analyze signals. It has a clear scheme, high efficiency, and it is perfect-reconstructive. In this section, a couple of important properties of Daubechies wavelet filters / Binomial QMF filters are discussed [12].

Let the scaling function (or father wavelet) of Daubechies wavelet is

$$\phi(n) = \{a_1, a_2, \dots, a_N\}\,, \tag{3.1}$$

where N is the length of the filter and a_i is scaling function coefficient. And define the wavelet function (or mother wavelet) is

$$\psi(n) = \{b_1, b_2, \dots, b_N\}\,, \tag{3.2}$$

where b_i is wavelet function coefficient. The scaling function coefficients satisfy the orthogonal property shown as the following.

$$\sum_{n\in Z} a_n a_{n+2m} = k\,\delta_{m,0}\,, \tag{3.3}$$

where m is any integer and k is a constant. It shows that the inner product of the scaling function coefficients with any odd-valued time shifting is zero, which describes the orthogonal property.

The relation between the scaling function coefficients and the wavelet function coefficients is

$$b_n = (-1)^n \cdot a_{N-n-1} \ , \tag{3.4}$$

where the order is reversed, and the signs are switched on odd indexes.

If Daubechies scaling and wavelet functions are used as filters, the scaling function is the low-pass filter and the wavelet function is the high-pass filter. The scaling and wavelet function coefficients are identical to the filter coefficients or impulse response. The filters are named as "DN" where *N* is the length of the filter response. D2 to D20 (even number indexes only) are typically used. The larger filter length gives the better edge of the frequency response.

The frequency response of Daubechies filters has a couple of interesting properties. First, their 3dB bandwidth is at the half of the highest frequency. In another word, the amplitude response gives $A/\sqrt{2}$ at middle of the analyzed frequency range, so it is half power at the middle frequency. This is the property for any filter length and for both low-pass and high-pass.

$$\left|H_0\left(\frac{\pi}{2}\right)\right| = \left|H_1\left(\frac{\pi}{2}\right)\right| = \frac{A}{\sqrt{2}}, \text{ and } \left|H_0\left(\frac{\pi}{2}\right)\right|^2 = \left|H_1\left(\frac{\pi}{2}\right)\right|^2 = \frac{A^2}{2}, \tag{3.5}$$

where H_0 and H_1 are respectively the frequency responses of the low-pass and high-pass filters, and *A* is the maximum magnitude of the frequency response.

The second property of frequency response is “mirror” property. The frequency magnitude responses of the low-pass and high-pass filters are symmetric with frequency. That is why they are called “mirror filters”.

$$|H_0(\omega)| = |H_1(\pi - \omega)|\,, \tag{3.6}$$

For instance of the two properties above, the figure below shows the magnitude responses of D6 (6-tap) filters.

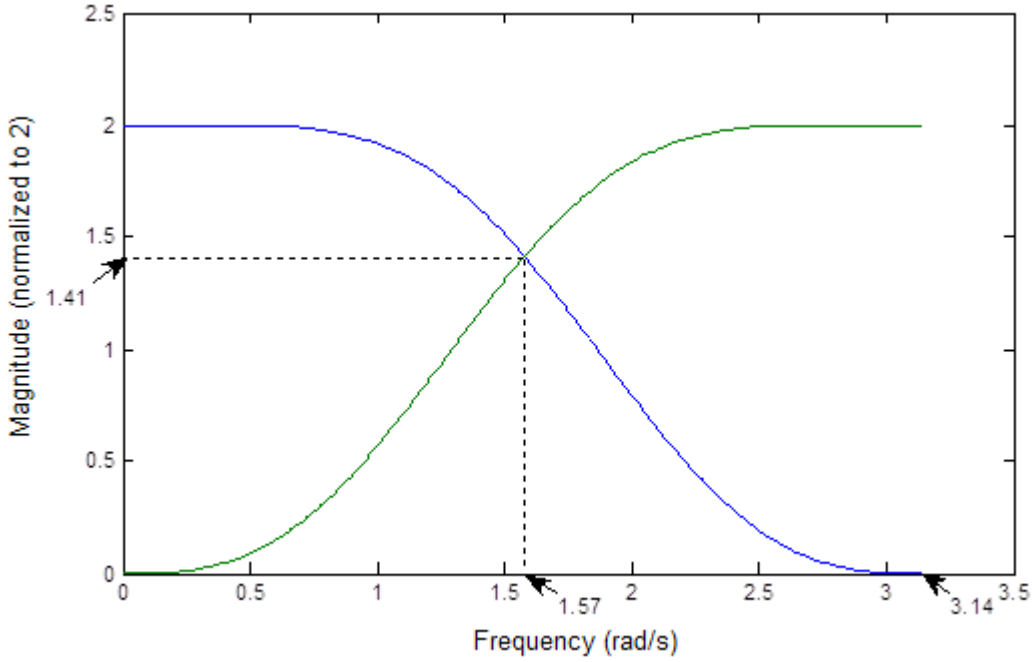

Figure 3.1 Magnitude-frequency responses of D6 low-pass and high-pass filters.

The last property of Daubechies filter to discuss in this section is about phase response. Daubechies filters are not accurately linear phase, but are approximately linear phase [16]. A little phase distortion may occur when signals passing through, but this will not affect the quality of analyzing and reconstructing. The figure below shows the phase responses of D6 low-pass and high-pass filters.

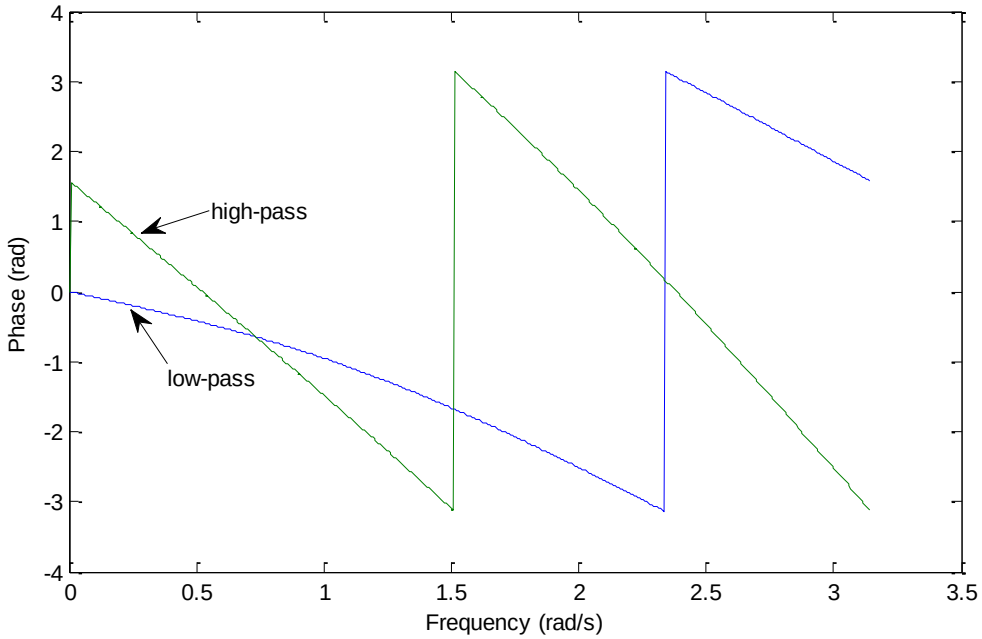

Figure 3.2 Phase-frequency responses of D6 low-pass and high-pass filters.

3.2 M-Band Subband Decomposition with Tree Structure [13]

As described in the last section, the low-pass and high-pass Daubechies filters have symmetric frequency responses. Thus, they can divide the input spectrum to two equal subbands called Low (L) band and High (H) band. And the low-pass and high-pass filters are a set of two-band quadrature mirror filter (QMF) bank. The L and H bands can again be applied to a two-band filter bank decomposition, and generate quarter bands: LL, LH, HL, and HH. These quarter bands can also be split to 8 subbands in the 3rd level, so on so forth. As needed in actual applications, input signals can be split to any number of subbands. They could contain a large range of frequency, or finely decompose the frequency components. This is an efficient multi-resolution analysis method using binary tree structure. If the binary tree is a complete tree, the subbands are evenly divided, and this method is called "regular" binary subband tree structure.

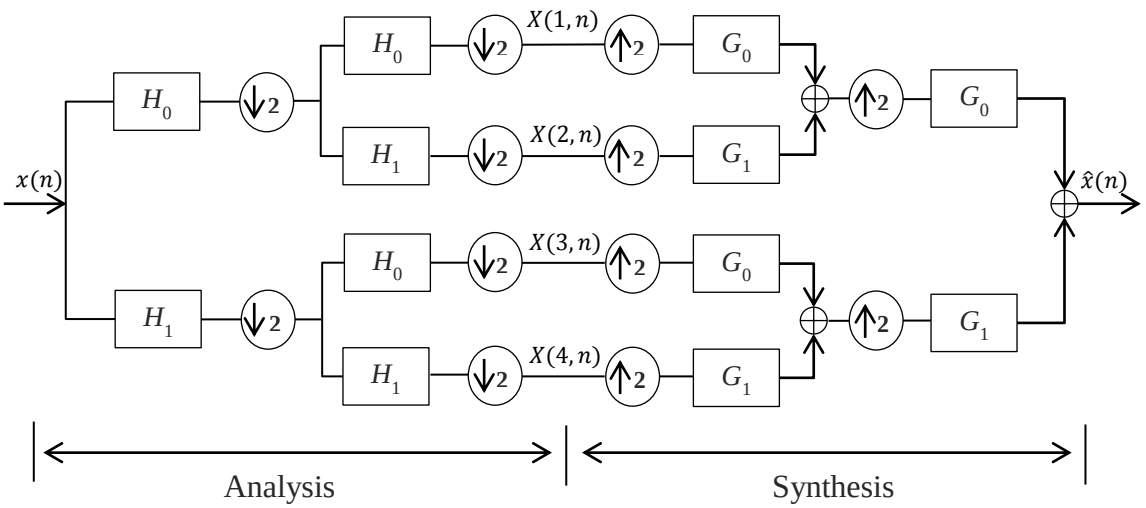

Figure 3.3 4-Band subband analysis and synthesis tree structure [13].

The decomposition tree structure is separated to analysis part and synthesis part. The analysis part functions as a forward transform that decomposes the input time domain signal $x(n)$ to frequency domain subbands $X(1,n),\dots,X(M,n)$. Unlike DFT, each subband component $X(k,n)$ has a sequence instead of just one point value. In the expression $X(k,n)$, *k* represents the index of subband, and *n* is a time index. The synthesis part, on the other hand, works as an inverse transform that recovers the subband sequences to time domain signal. If perfect-reconstruction quadrature mirror filter banks (PR-QMF) are employed, the reconstructed signal $\hat{x}(n)$ is exactly the same as the input $x(n)$ except some delay.

The subband decomposition scheme is constructed by PR-QMFs and binary tree structure. In a "regular" subband structure, *M* subbands are decomposed, for any positive integer *N*, and $M = 2^N$. The two-band PR-QMFs are set to each branch of the binary tree shown in Figure 3.3. The analysis filters (H_0 ,H_1) and synthesis filters (G_0 , G_1) are used to decompose and reconstruct signals. All of them are PR-QMFs and they are generated from

the coefficients that satisfy the perfect-reconstruction conditions. Daubechies filters / binomial QMF filters are good examples of PR-QMFs and match these conditions.

It has been proved that the two-band PR-QMFs with length *N* satisfy the following conditions:

$$\rho(2n) = \sum_k h_0(k) \cdot h_0(k+2n) = \delta(n)\ , \tag{3.7a}$$

$$H_1(z) = z^{-(N-1)} H_0(-z^{-1})\ , \tag{3.7b}$$

$$G_0(z) = z^{-(N-1)} H_0(z^{-1})\ , \tag{3.7c}$$

$$G_1(z) = z^{-(N-1)} H_1(z^{-1})\ . \tag{3.7d}$$

Equation (3.7a) is equivalent to Equation (3.3), which is the orthogonal condition of Daubechies scaling function. Therefore, Daubechies low-pass filter satisfies the PR-QMF condition of filter h_0. The other three filters can be easily got by (3.7b)-(3.7d). These equations can be converted to time domain by inverse Z-transform:

$$h_1(n) = (-1)^{n-1}\, h_0(N-n-1)\ , \tag{3.8a}$$

$$g_0(n) = h_0(N-n-1)\ , \tag{3.8b}$$

$$g_1(n) = (-1)^n\, h_0(n)\ . \tag{3.8c}$$

Equation (3.8a) is equivalent to Equation (3.4), which is the relation between Daubechies scaling function and wavelet function. The coefficients of h_1 and the wavelet function (high-pass filter) have opposite values, but their frequency responses are the same. Thus, Daubechies high-pass filter can be used as filter h_1 after taking opposite values. Filter g_0 and g_1 are also easy to get by relations (3.8b) and (3.8c).

Down-sampling and up-sampling are important to keep the appropriate sampling rate of each signal in analysis and synthesis processes. In analysis part, signals are down-sampled by 2 at each output of filters. On the contrary, in synthesis part, signals are

up-sampled by 2 at each input of filters. Each analysis or synthesis level has different sampling rate, but the changed rates are just appropriate for the filtering processes. These down-samplings and up-samplings can keep the analysis and synthesis processes making full use of the re-sampled spectrum. Furthermore, due to the down-samplings in the analysis part, the signals passed through high-pass filters have reversed spectrums in the analyzed subband. Because of this spectrum reversion, a mapping from subband index to frequency index is required when considering equalization. This is a point discussed in the next section.

In many applications, frequency intervals of the overall spectrum are not equally important or significant. For example, a channel might be approximately flat-fading in low frequency area, but frequency-selective in high frequency area. We prefer finer frequency resolution for frequency-selective area than flat-fading area. In order to decrease the computational complexities of analysis and synthesis operations, one can combine some subbands (like the flat-fading area) in the decomposition binary tree and yield larger bandwidth subbands. In Figure 3.4 as an example, subbands k=3 and k=4 in the "regular" scheme are combined to a larger bandwidth subband k=3. It is an important idea of multi-resolution analysis that subbands have unequal bandwidths according to different resolution requirements. This method is called "irregular" binary subband tree structure, contrasting "regular" structure with equal bandwidths. But as common, both of the regular and irregular structures split the spectrum as a power of 2, since they repeatedly employ a 2-band filter bank. The spectrum separation of subbands is shown in Figure 3.5, assuming the filters are ideal low-pass or high-pass. Each subband sequence $X(k,n)$ represents the signal component in the bandwidth that it occupies.

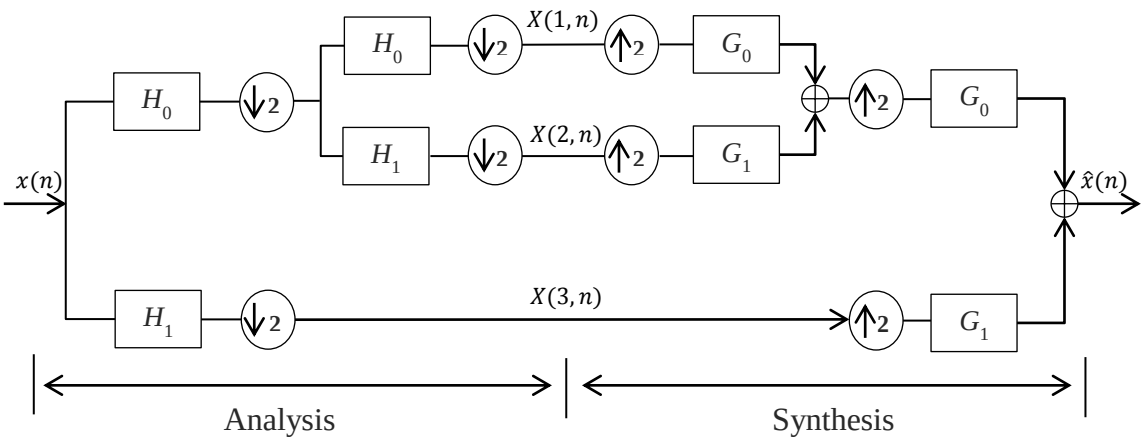

Figure 3.4 3-Band irregular analysis and synthesis tree structure.

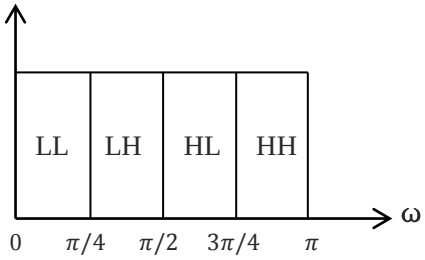

Figure 3.5(a) Regular tree 4-band splitting.

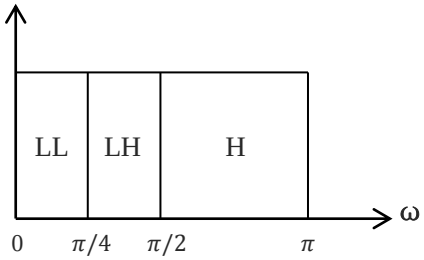

Figure 3.5(b) Irregular tree 3-band splitting.

3.3 Subband-Based Frequency Domain Equalization

In this section, the subband decomposition technique is employed to frequency domain equalization (FDE) that discussed in section 2.4. This method is an expansion to the basic FDE scheme (Figure 2.2). Three changes are made in the basic FDE scheme to give the subband equalization scheme: "Forward Transform" block is replaced by subband analysis; "Inverse Transform" block is replaced by subband synthesis; and the frequency components $X(k), Y(k)$ are replaced by subband sequences $X(k,n), Y(k,n)$.

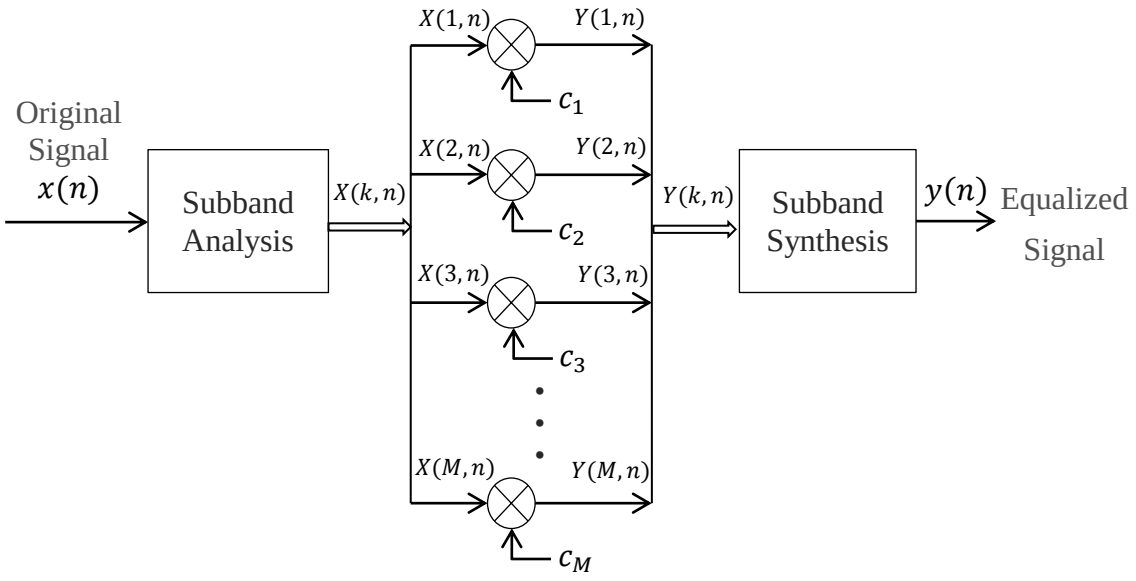

Figure 3.6 Subband equalization block diagram.

The equalizer coefficients $c_1, \ldots, c_M$ are used to compensate the frequency response of the channel, multiplying with subband sequences $X(1,n), \ldots, X(M,n)$.

$$Y(k,n) = X(k,n) \cdot c_k \,, \tag{3.9}$$

where *k* is the index of the subband to be equalized. The *k*th subband represents the signal component in its spectrum bandwidth, which is determined by the splitting way of the tree structure.

It is very important to notice that the subband sequences $X(1,n), \ldots, X(M,n)$ are not in the order of frequency, but have a mapping from subband index to frequency index. The equalizer coefficients $c_1, \ldots, c_M$ are not in the order of frequency either, but are mapped from the frequency domain coefficients. The reason for that is the spectrum reversion caused by the down-sampler in the analysis process. Each signal passed through a high-pass filter and down-sampled by two has a reversed spectrum. The low-pass filtering on this signal is equivalent to high-pass filtering on the actual spectrum. Similarly,

high-pass filtering on this signal is equivalent to low-pass filtering on the actual spectrum, due to its reversed spectrum. Therefore, the mapping from subband index to frequency index is shown in the figure below, in which the reversed bands are marked as bold.

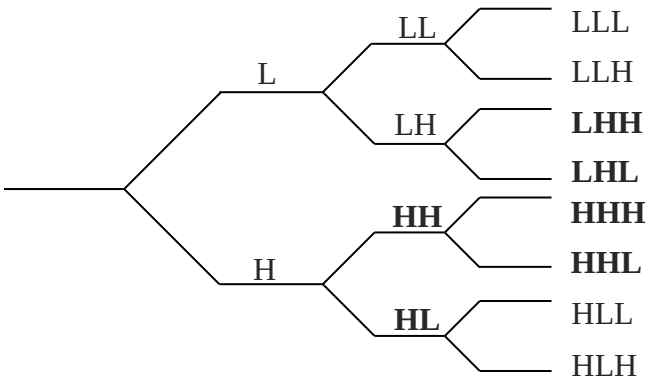

Figure 3.7 Mapping from subband index to frequency domain bands.

Subband equalizers can be more flexible and efficient than a basic equalizer by choosing the use of regular structure or irregular structure. If the frequency response of a channel changes a lot in a certain bandwidth, a finer resolution of analysis is needed to make the analysis accurate enough. On the other hand, if the frequency response doesn't change much in that bandwidth, lower resolution is good enough, and less filter banks are needed in this band. Thus, an irregular structure can make such kind of efficient subband splitting, which saves the computational time and system resources in an actual application. This method is called "multi-resolution equalization".

To give an example of multi-resolution equalization, assume a linear time-invariant (LTI) channel with impulse response $h(n)$, with arbitrary coefficients.

$$h(n) = \{0.7,0.4,0.8,0.2\} \tag{3.10}$$

The received signal passing through the channel is given by the convolution of the transmitted signal and the channel impulse response.

$$r(n) = t(n) * h(n) \tag{3.11}$$

And the received spectrum equals the transmitted spectrum multiplied by the channel frequency response.

$$R(\omega) = T(\omega)H(\omega) \tag{3.12}$$

where $H(\omega)$ is the Fourier transform of $h(n)$. The magnitude-frequency response $|H(\omega)|$ of the channel is plotted with the subband splitting.

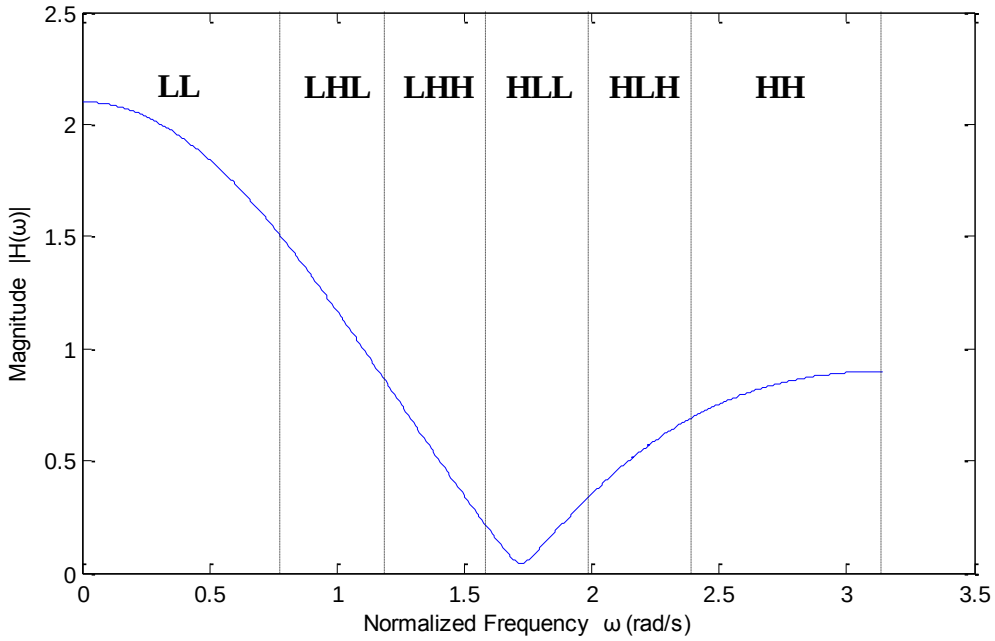

Figure 3.8 Magnitude-frequency response with subband splitting.

As an example of the irregular subband splitting, the entire bandwidth is split into six subbands with two different resolutions. In the bands that the frequency response changes "faster", the finer resolution is used (like LHL, LHH, HLL, and HLH subbands). Otherwise, the lower resolution is used (like LL and HH subbands). Using an irregular tree structure in Figure 3.4, this subband splitting can be completed with a 3-level structure. Then, employ this band splitting into the subband equalization scheme (Figure 3.6).

CHAPTER 4

OPTICAL WIRELESS TRANSMISSION SCHEME

4.1 IM/DD DOW Communication System

Diffuse optical wireless (DOW) communication system employs infrared or other optical signals to transmit data symbols. The word "diffuse" means the beans of optical signals are not concentrated like laser, but have multiple directions of reflections. As described in Figure 1.1, the electronic signal is converted to optical signal by LEDs, and then converted back to electronic signal by photodiodes.

"Intensity modulation and direct detection" (IM/DD) is a basic transmission scheme used in DOW, which indicates that the optical signal is modulated and detected by the transmitted power [2]. Therefore, the requirement of IM/DD is that the transmitted signal must be real and non-negative, because power is always real and non-negative. But the thing is mostly the modulated signal has positive and negative parts, like QPSK signals. Also, in Chapter 2 and Chapter 3, the transmitted signals are real but not non-negative. Something needs to be done before output them to the LED.

The first way that easy to imagine is adding a DC component to the transmitted signal to make it non-negative.

$$t'(n) = t(n) + |\min\{t(n)\}| \tag{4.1}$$

This method could work but it's not efficient, because it enlarges the dynamic range of the transmitted signal and put more signal parts to the non-linear range of LEDs. To avoid non-linear distortion, the only way could do is compress the amplitude of the signal and decrease the amplitude resolution. It's not ideal.

4.2 Decomposed Non-Negative Transmission

The second way to make a non-negative signal is to decompose the transmitted signal to positive and negative parts, reverse the negative part, and transmit them separately with two time slots [1]. This is called "decomposed non-negative transmission".

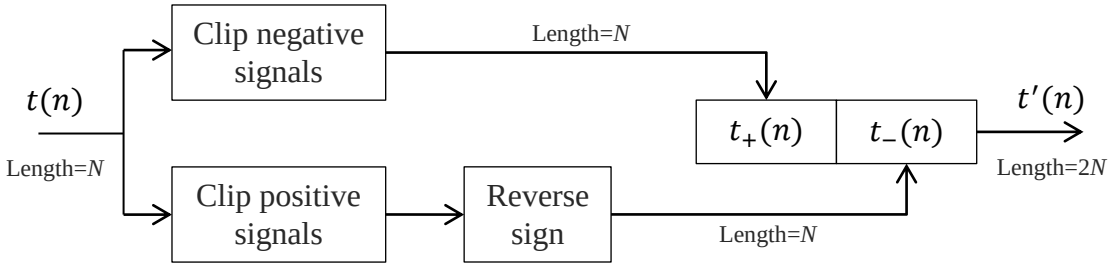

Figure 4.1 Block diagram of a basic decomposed non-negative transmission.

$$t_+(n) = \begin{cases} t(n), & if\ \ t(n) > 0 \\ 0, & if\ \ t(n) \le 0 \end{cases} \tag{4.2a}$$

$$t_-(n) = \begin{cases} 0, & if\ \ t(n) > 0 \\ -t(n), & if\ \ t(n) \le 0 \end{cases} \tag{4.2b}$$

$$t'(n) = \begin{cases} t_+(n), & if\ \ 0 \le n < N \\ t_-(n), & if\ \ N \le n < 2N \end{cases} \tag{4.2c}$$

This transmission scheme uses separated positive and negative time slots to represent the transmitted signal (shown in Figure 4.1 and Equation 4.2). The dynamic range doesn't change and the transmitted signal is recoverable. But in this scheme, the usage of time slots is not efficient. Only 50% of time is used to transmit signal, and the other half of time is "blank" (zero amplitude). The positive signal time slots cut off the negative signals to zero, and the negative slots cut off the positive signals. There is naturally "blank" (zero) in 50% of transmission time.

To make an improvement on time efficiency, just remove some useless “blanks” in the transmitted signal. The purpose of the “blanks” is to indicate the positions of negative signals or positive signals. They don’t need to happen twice. Just remove the “blanks” in the negative slots (or positive slots). After the removal, the positive and negative signals are still easy to get recovered, and only $1/3$ of the transmission time is “blanks” (zeros) rather than $1/2$. The efficiency has an improvement of 33.3% than the original scheme. In the simulation chapter, an example of the transmitted signal is shown.

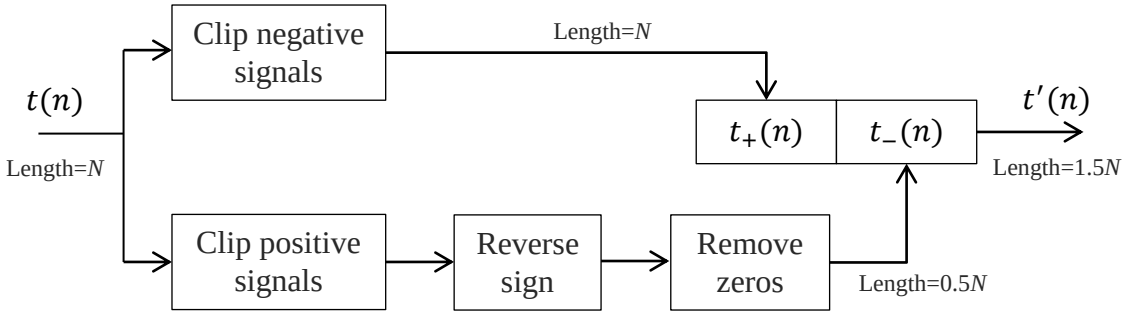

Figure 4.2 Block diagram of the decomposed non-negative transmission with zeros removal.

4.3 Overall Transmission Scheme

This overall transmission scheme combines all of the blocks discussed in the previous sections and chapters.

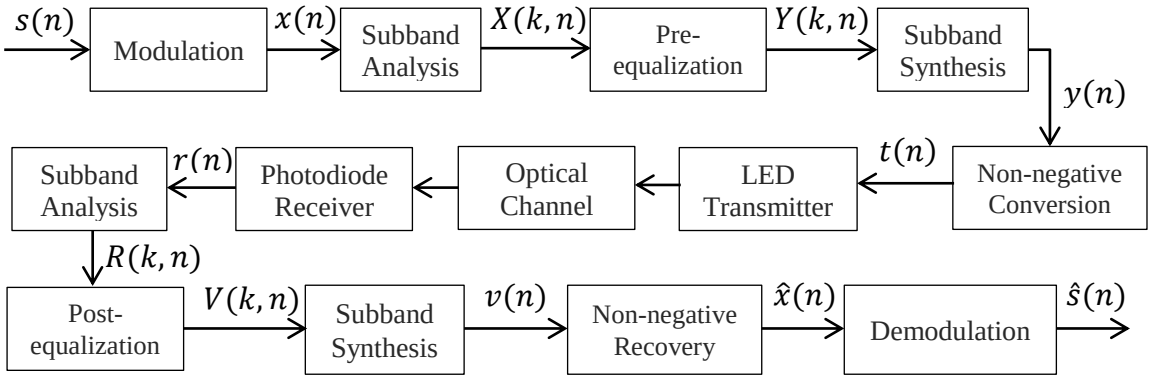

Figure 4.3 Block diagram of the overall transmission scheme.

CHAPTER 5

SIMULATIONS

5.1 Modulation and Detection

In this set of simulation, quadrature phase shift keying (QPSK) and quadrature amplitude modulation (QAM) are used to generate modulated sequences with arbitrary symbols. Matched filtering detector is employed to detect symbols from the received and equalized sequence.

Figure (5.1) shows the modulated QPSK and 64-QAM sequence with arbitrary input symbols. Figure (5.2) shows the detected constellation from long QPSK and 64-QAM sequences by a matched filtering detector.

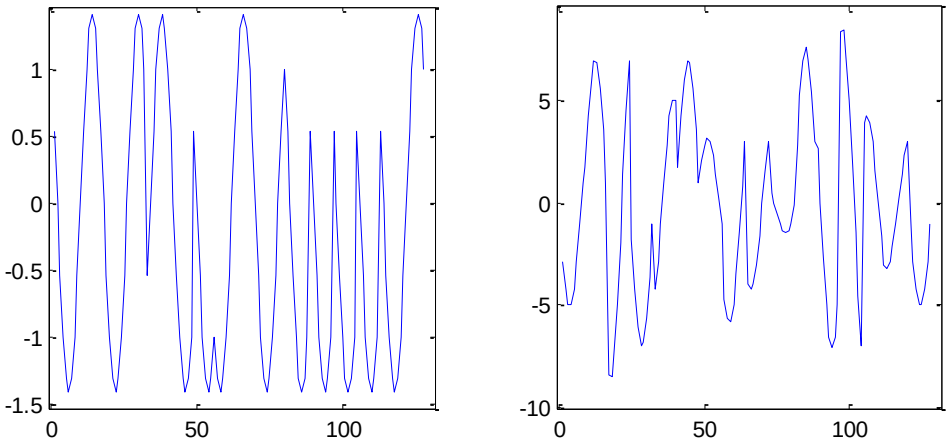

Figure 5.1 (a) QPSK modulated sequence. (b) 64-QAM modulated sequence.

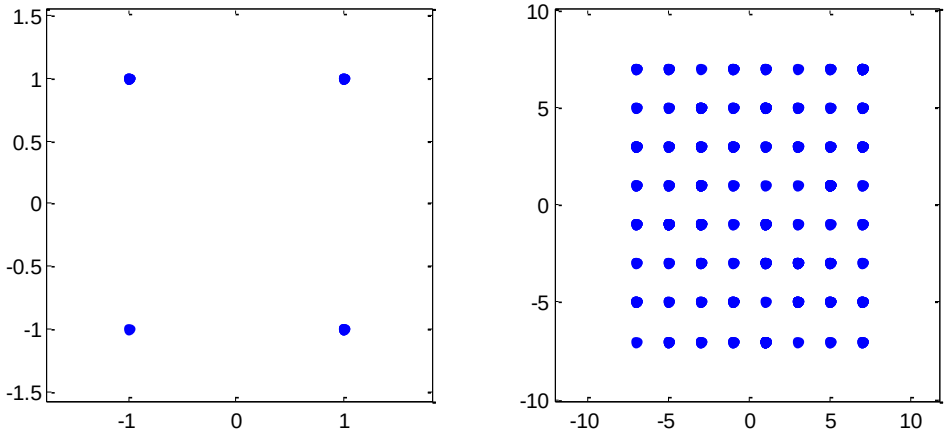

Figure 5.2 (a) Detected QPSK constellation. (b) Detected 64-QAM constellation.

For the figures in this chapter, if a time-domain signal is shown, X-axis represents discrete time index and Y-axis represents signal amplitude; if a frequency-domain spectrum is shown, X-axis represents normalized frequency and Y-axis represents magnitude or phase; if a constellation is shown, X-axis represents in-phase values and Y-axis represents quadrature values.

5.2 Subband Analysis and Synthesis

Subband decomposition technique employs binomial-QMF banks to decompose time-domain signals to frequency-domain subbands, and perfectly reconstruct the time-domain signals. Subband analysis and synthesis are essential processes of subband-based FDE.

In the following simulation, a QPSK signal is used as the input, and it is decomposed into four subband components by the analysis process. Then, from the subband components, the original signal is recovered by the synthesis process. The reconstructed signal is the same as the input, except some delay and different amplitude

normalization. The perfect-reconstruction property is demonstrated from that. The time delay of the reconstructed signal is given by

$$N_D = (M-1)\cdot(L-1)\,, \tag{5.1}$$

where M is the number of analyzed subbands, and L is the length of the QMF filter.

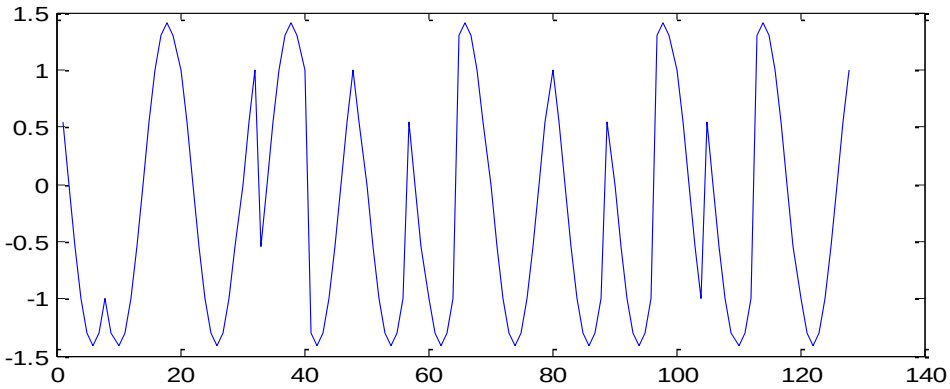

Figure 5.3 Input QPSK signal.

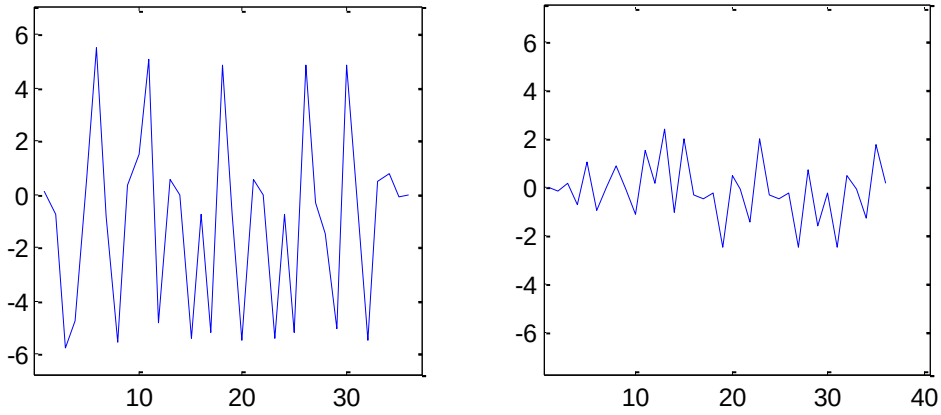

Figure 5.4 (a) Subband sequence $X(1, n)$. (b) Subband sequence $X(2, n)$.

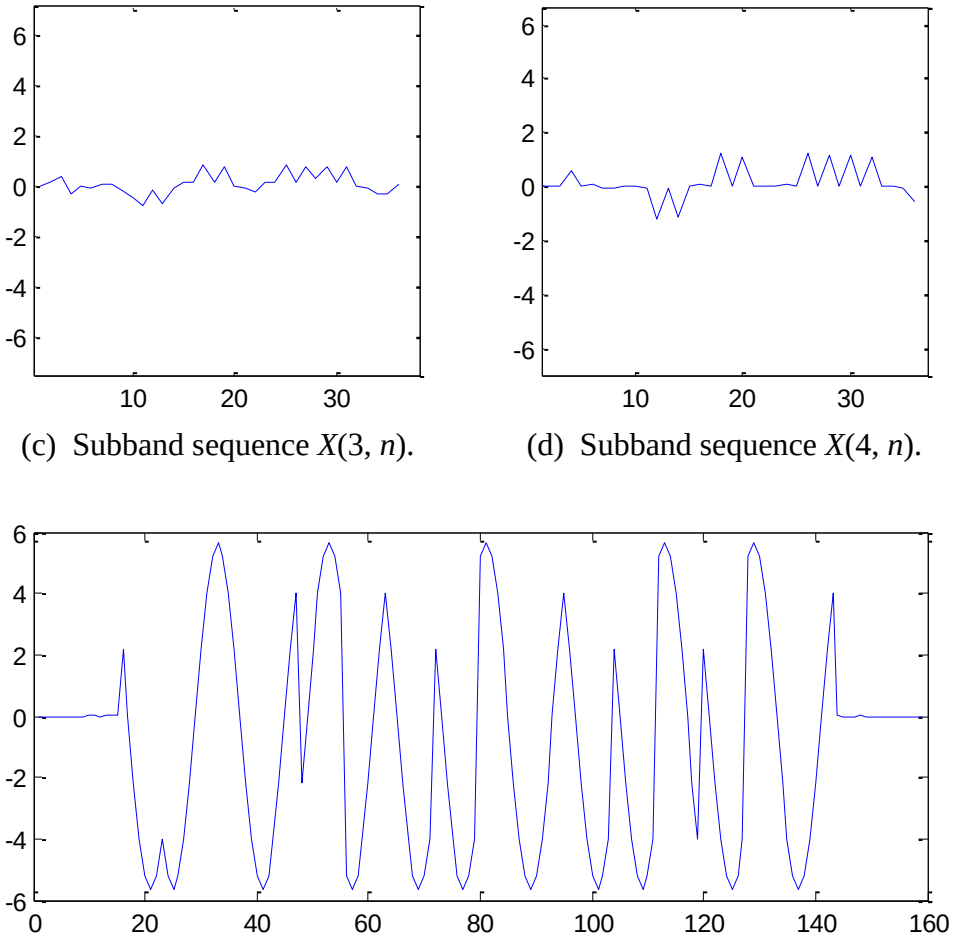

(c) Subband sequence $X(3, n)$. (d) Subband sequence $X(4, n)$.

Figure 5.5 Reconstructed (synthesized) signal – the same as the input with some delay.

5.3 Decomposed Non-Negative Conversion and Recovery

In this section, the simulation on "decomposed non-negative transmission" scheme is demonstrated. This simulation compares the converted non-negative signals with the recovered signal. Both regular and zero-removal schemes are used to generate non-negative signals.

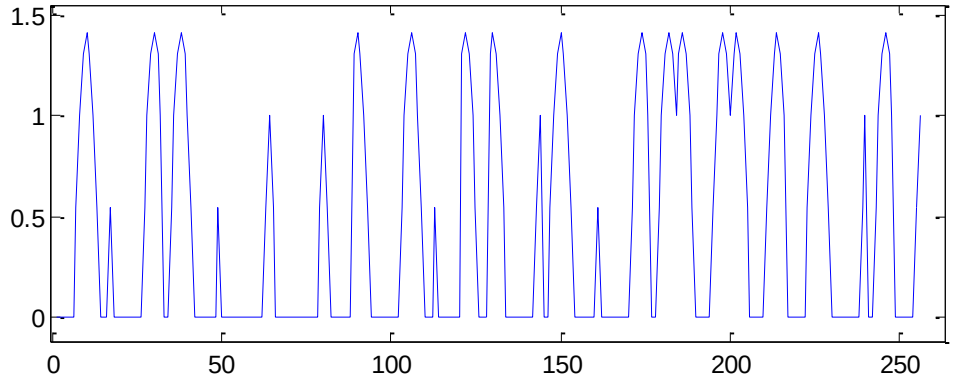

Figure 5.6 Regular decomposed non-negative transmitted signal.

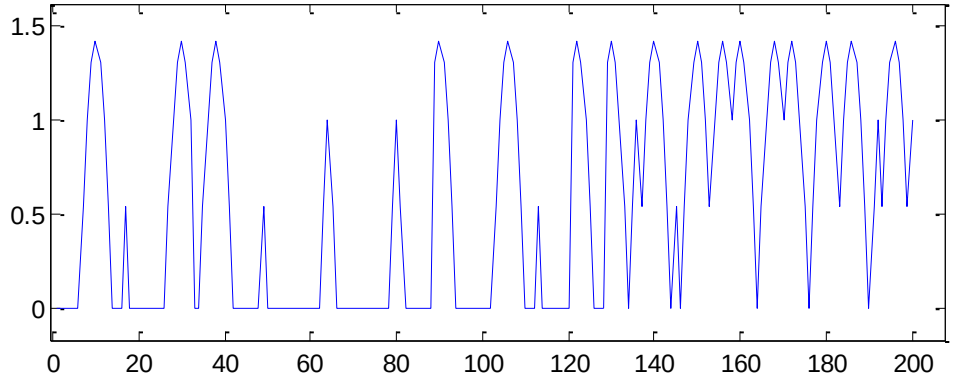

Figure 5.7 Zero-removal decomposed non-negative transmitted signal.

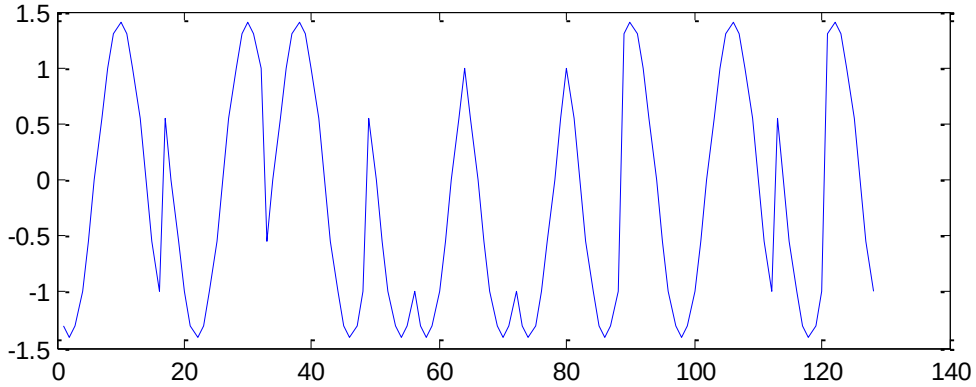

Figure 5.8 Recovered transmitted signal.

5.4 SCFDE Simulation

In this section, the simulation on subband-based SCFDE is given. Assume the transmitted signal passes through a designated channel. The performances of five equalization methods and a non-equalization method are compared in this set of simulations.

1. Channel Description

The channel model used for this simulation is a frequency selective channel with additive white Gaussian noise (AWGN). The signal-to-power ratio (SNR) is designated as 15dB or variant values.

The impulse response of the channel is

$$h(n) = \{0.8, 0.4, 0.2, 0.1\} . \quad (5.2)$$

The magnitude and phase frequency response of this channel is shown in Figure 5.9. It is obvious that the channel is frequency-selective, because the attenuation is much greater in higher frequency than in lower frequency. This channel is also multipath, with four echoes (4-tap response). Therefore, ISI may occur to the transmitted signal.

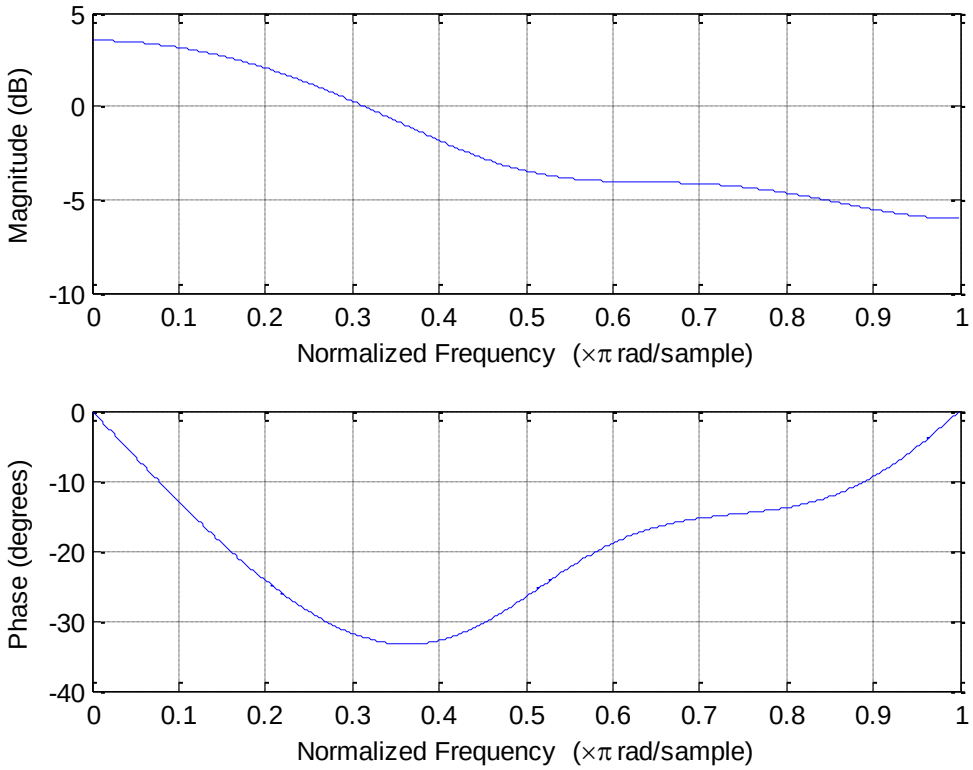

Figure 5.9 Frequency response of the channel.

2. The Detection without any Equalization

In this simulation, the demodulator directly detects the received signal passed through the channel without any equalization. In the following figures, the transmitted and received signals, as well as the spectra, are compared and shown. The received signal is distorted on edges and turns in the waveform, and the higher frequency spectrum is more attenuated than the lower frequency spectrum. The detected constellation is shown at last, where the points are dispersed. Thus, the detected symbols are very likely to be error.

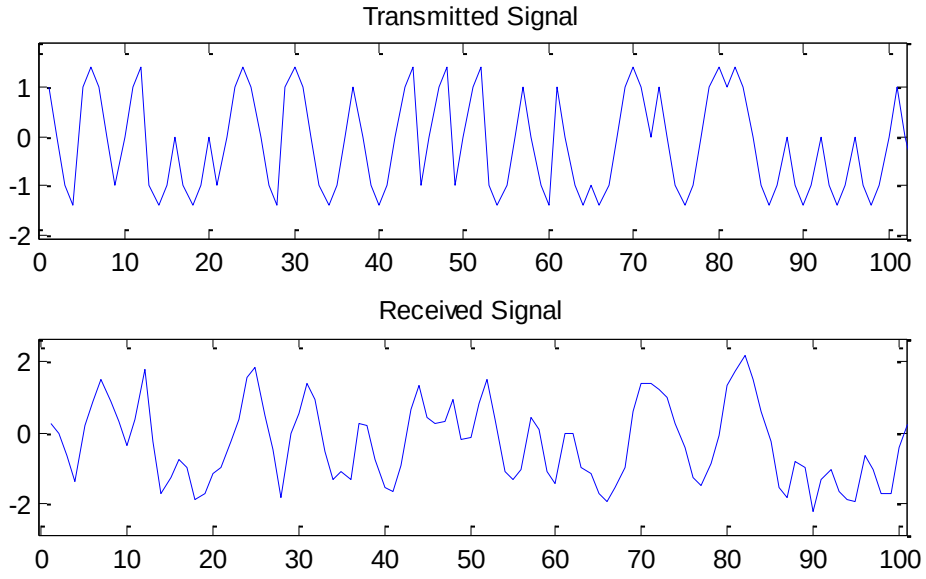

Figure 5.10 Transmitted signal and received signal without equalization (15dB SNR).

The transmitted spectrum and the received spectrum are compared in Figure 5.11.

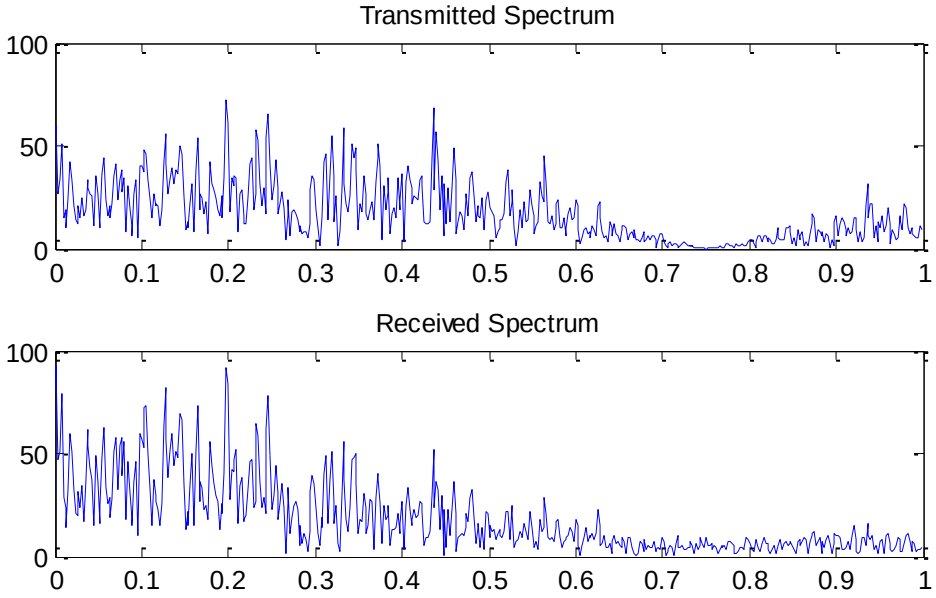

Figure 5.11 Transmitted and received spectra without equalization (15dB SNR).

The received constellation is shown in Figure 5.12.

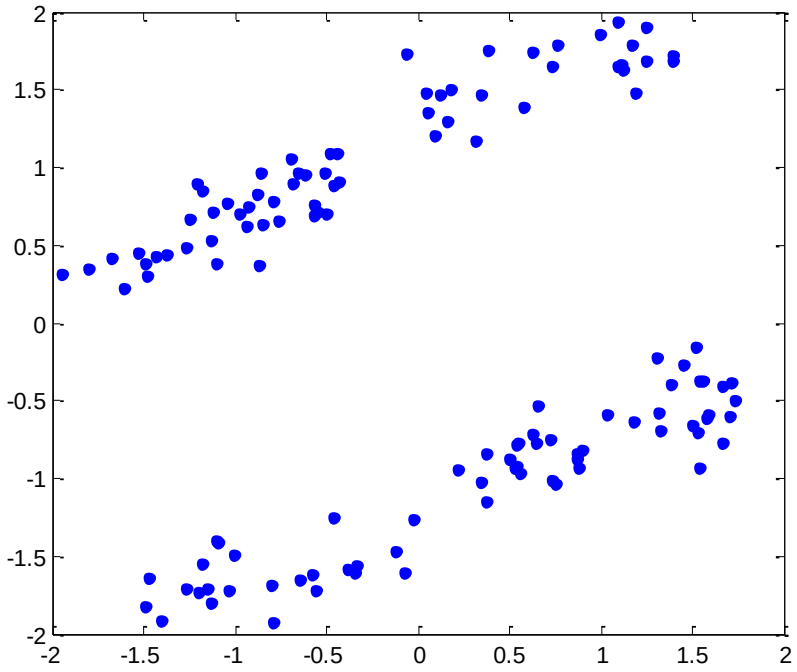

Figure 5.12 Constellation of the received signal without equalization (15dB SNR).

3. The Fine Post-equalization

In this simulation, the transmitter doesn't contain a pre-equalizer, but the receiver contains a post-equalizer with a fine frequency resolution (64-subband). The post-equalizer is able to compensate the frequency selective distortion in the received signal.

The equalized signal has recovered and enhanced edges and corners, which are likely to be distorted in the channel. In the equalized spectrum, the higher frequency components are enhanced to compensate the frequency selective attenuation. The equalized constellation is shown to be more concentrated than the constellation without any equalization. Thus, fewer errors may occur.

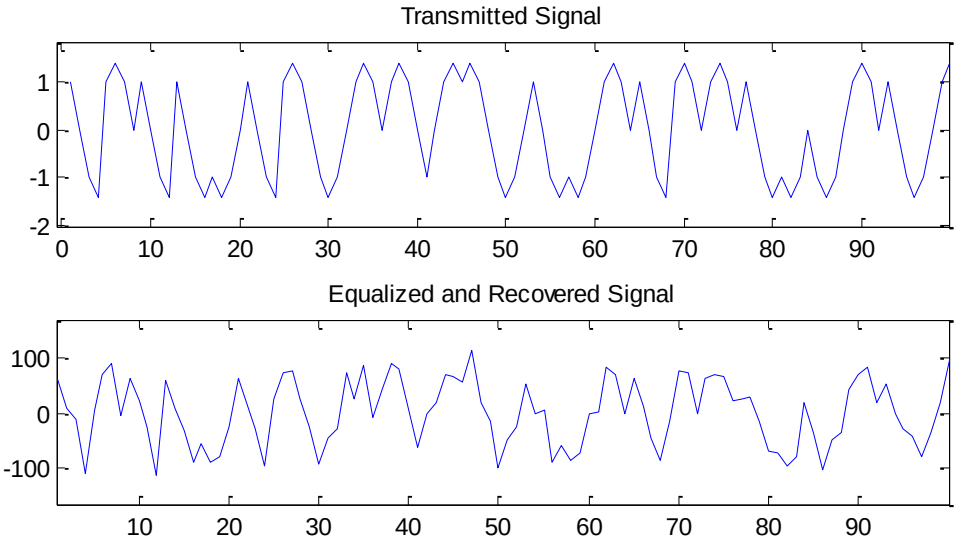

Figure 5.13 Transmitted signal and recovered signal with post-equalization (15dB SNR).

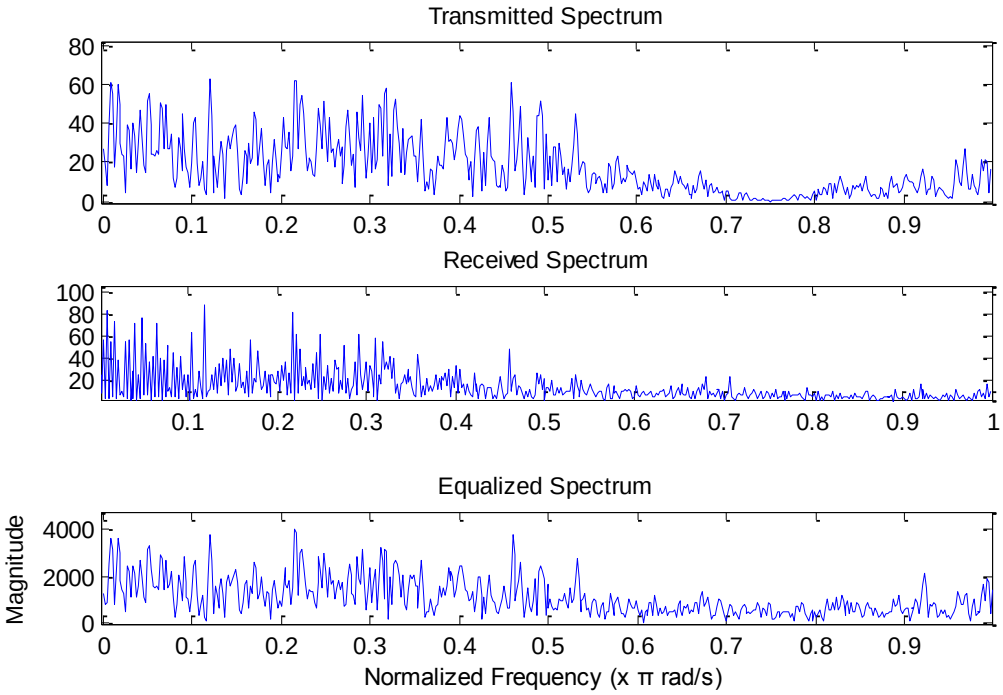

Figure 5.14 Spectra comparison (15dB SNR).

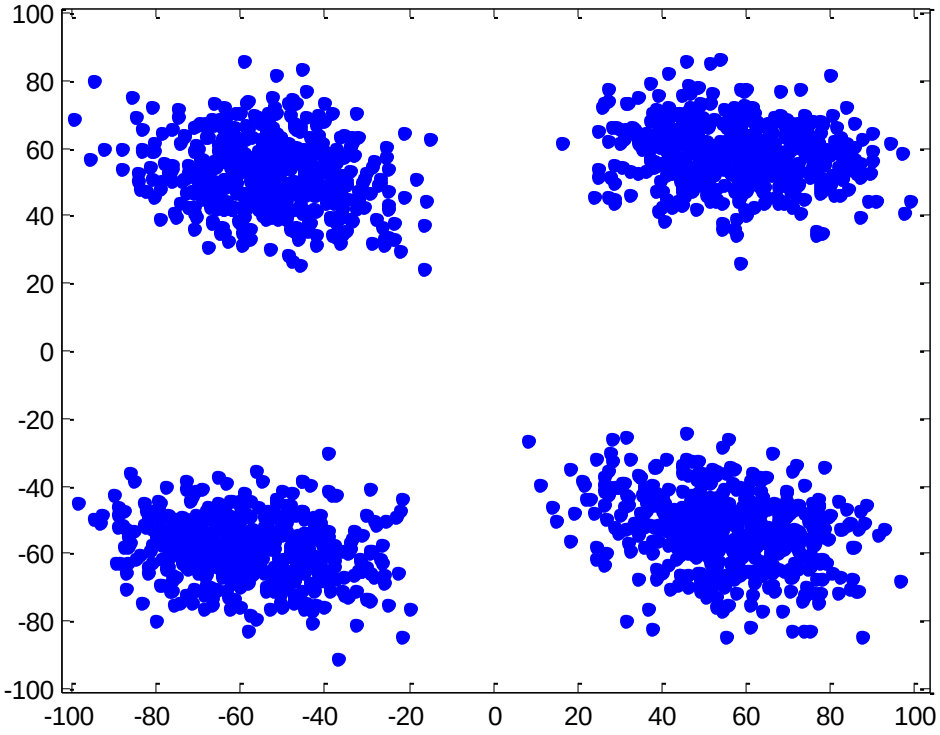

Figure 5.15 Equalized constellation with fine post-equalization (15dB SNR).

4. The Rough Post-equalization

This simulation has the same scheme as a fine post-equalization, except using a rough post-equalizer with only two subbands. This can save some computational cost than using a fine post-equalizer, but the performance may be not as good as a fine equalizer.

Figure 5.16 shows the comparison of the transmitted signal and the recovered equalized signal.

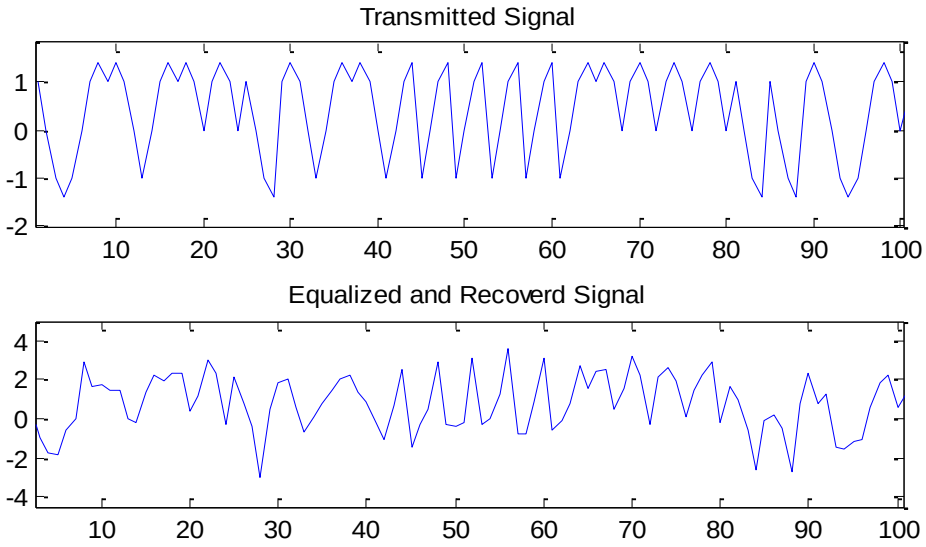

Figure 5.16 Transmitted signal and equalized signal with rough post-equalization.

The transmitted spectrum, the received spectrum, and the equalized spectrum are compared in Figure 5.17.

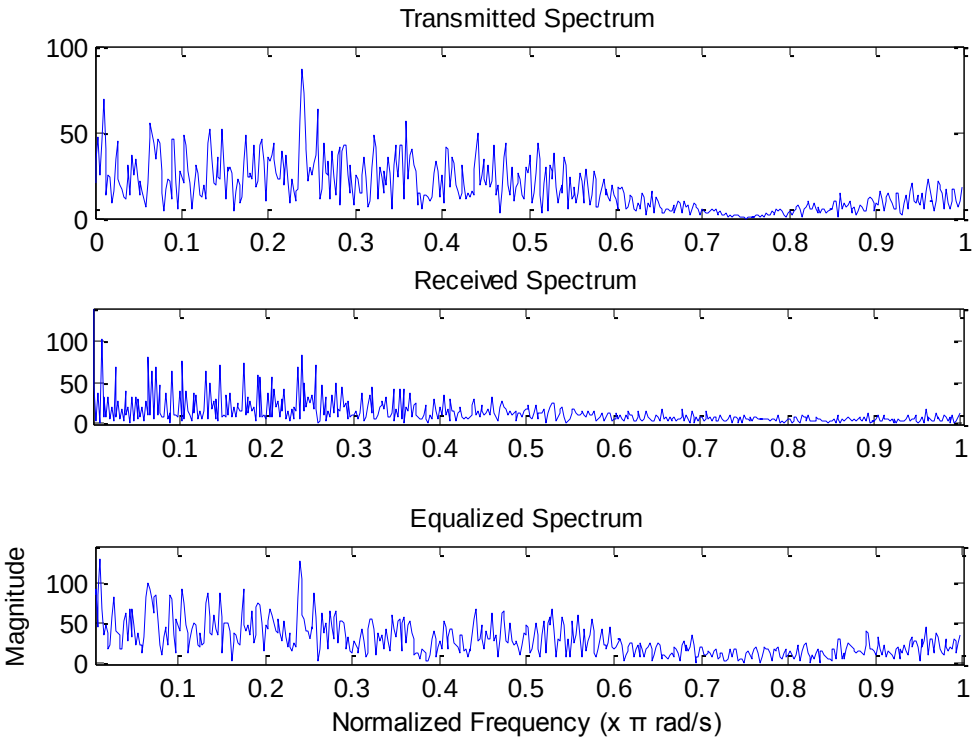

Figure 5.17 Spectra comparison.

The equalized constellation is shown in Figure 5.18. It is more concentrated than the constellation without any equalization but not as good as the performance of a fine equalizer.

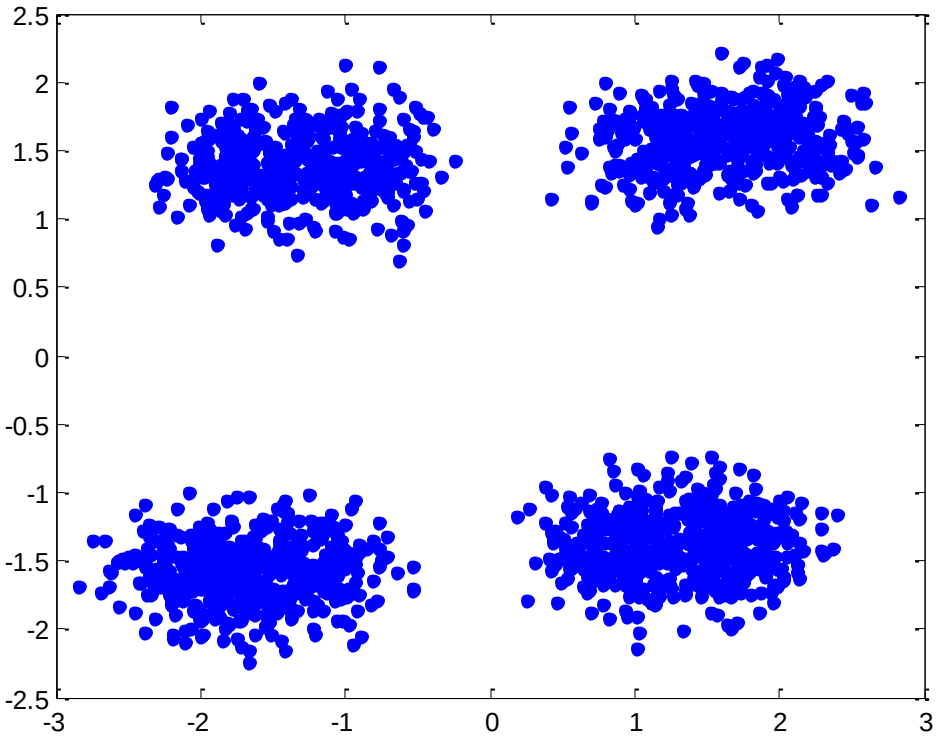

Figure 5.18 Constellation of the equalized signal.

5. Fine Pre-equalization

In this simulation, the transmitter contains a pre-equalizer, and the receiver detects the symbols directly without equalization. Pre-equalizer modifies the transmitted signal in its spectrum to compensate the frequency selective fading of the channel. The pre-equalized signal has enhanced higher frequency components to compensate the attenuation in the channel. Pre-equalization may have better performance than post-equalization, because the transmitted signal is equalized before the white noise added to the received signal. In other words, pre-equalization performs on a noise-free signal

while post-equalization works on a signal with AWGN. But a disadvantage of pre-equalization is a little higher PAPR due to the enhanced high frequency components.

The transmitted signal and the received signal are compared in Figure 5.19.

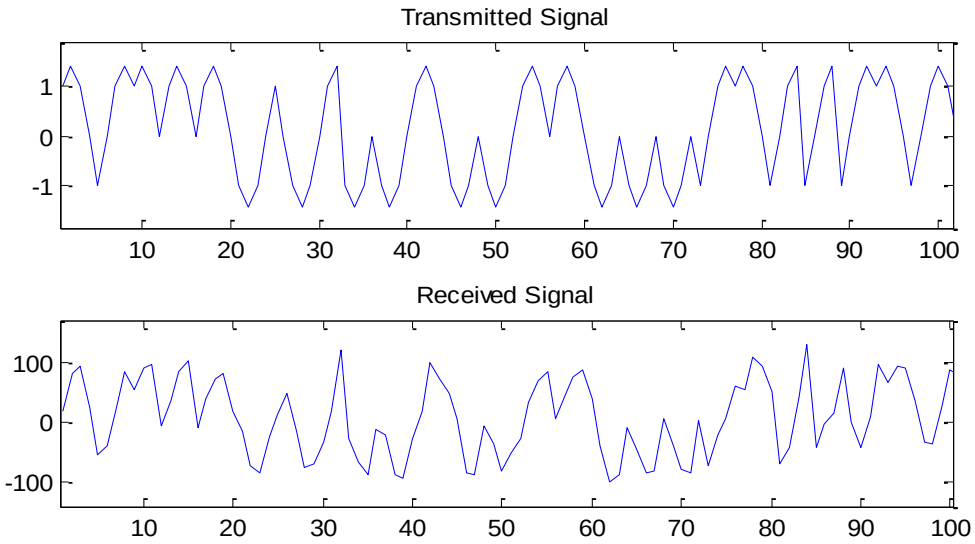

Figure 5.19 Transmitted signal and received signal with fine pre-equalization.

The transmitted spectrum, pre-equalized spectrum, and the received spectrum are shown in Figure 5.20.

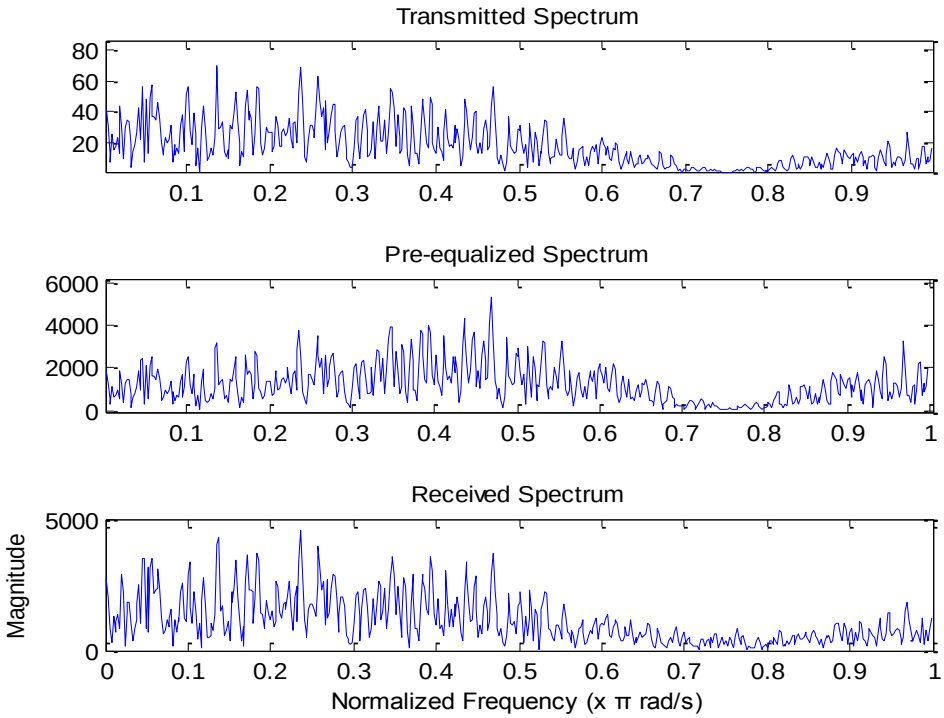

Figure 5.20 Spectra comparison.

The received constellation with pre-equalization is shown in Figure 5.21.

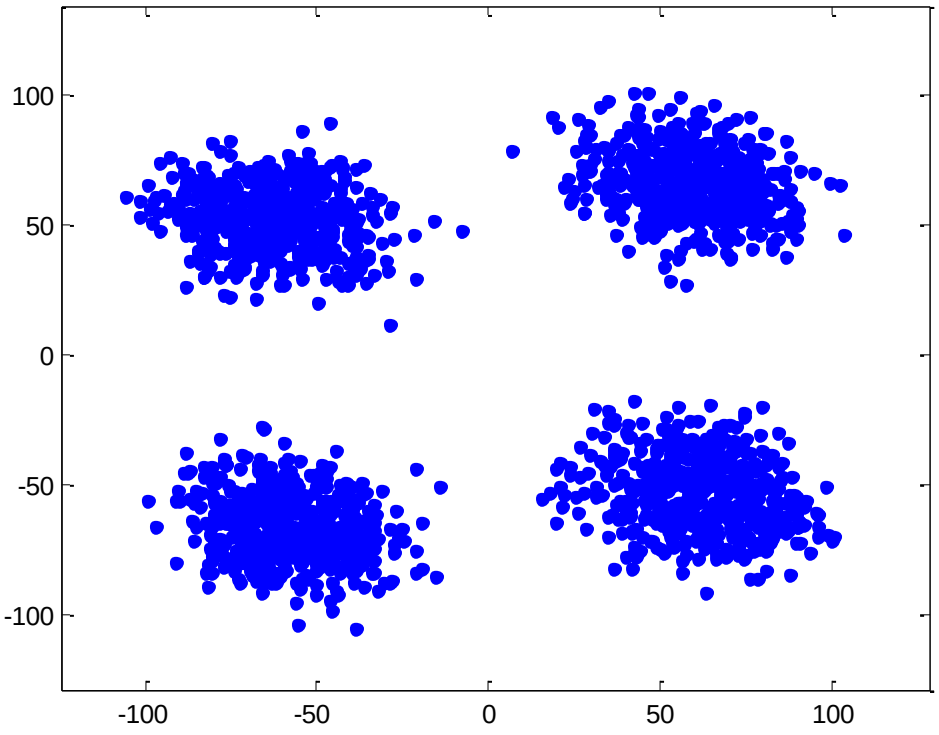

Figure 5.21 Received constellation with fine pre-equalization.

6. The Rough Pre-equalization

This simulation has the same scheme as the fine pre-equalization, except using only two-band decomposition.

The transmitted signal and the received signal are plotted and in Figure 5.22.

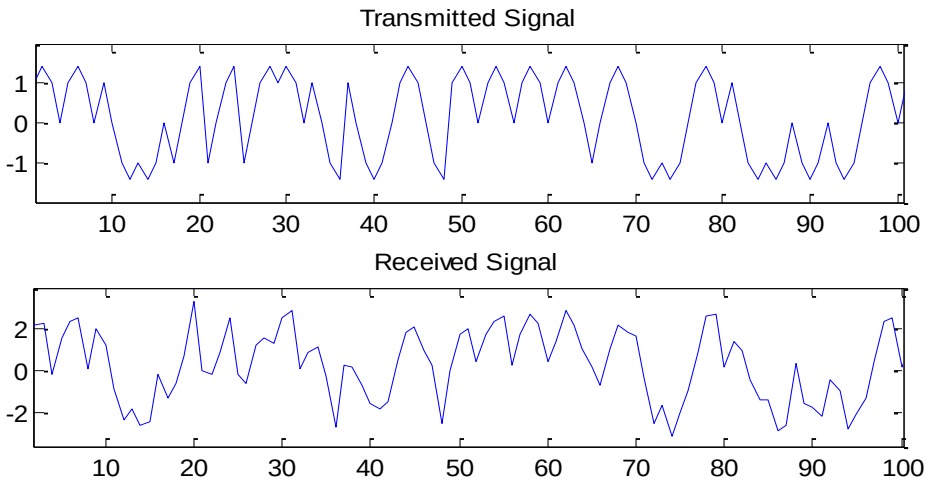

Figure 5.22 Transmitted signal and received signal with rough pre-equalization.

The transmitted spectrum, the roughly pre-equalized spectrum, and the received spectrum are compared in Figure 5.23.

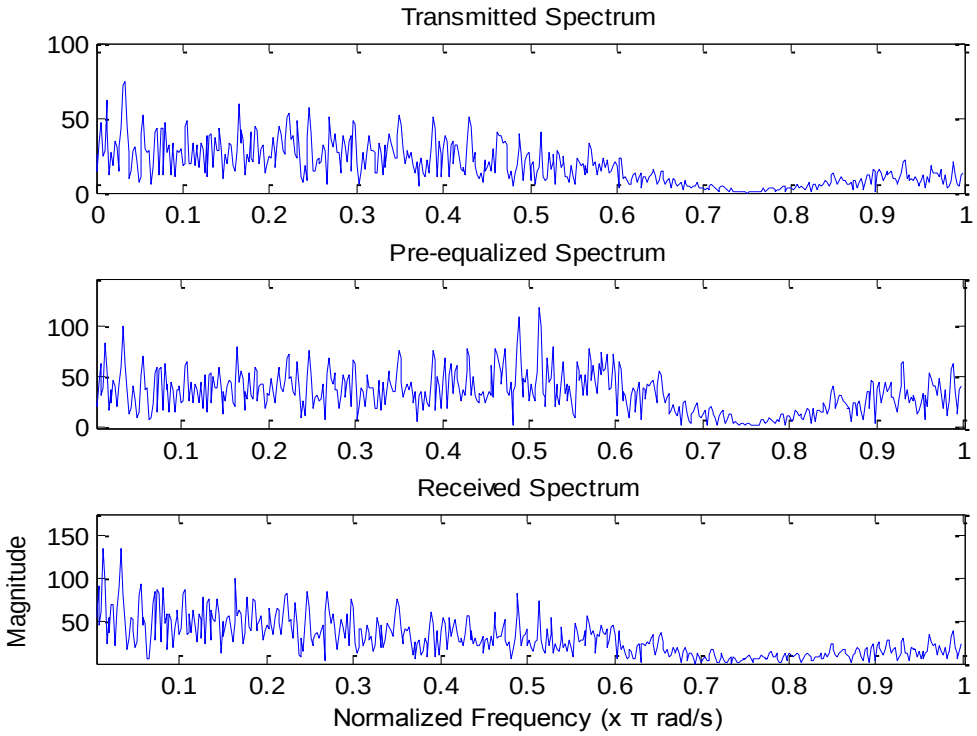

Figure 5.23 Spectra comparison.

The received constellation with the rough pre-equalization method is shown in Figure 5.24.

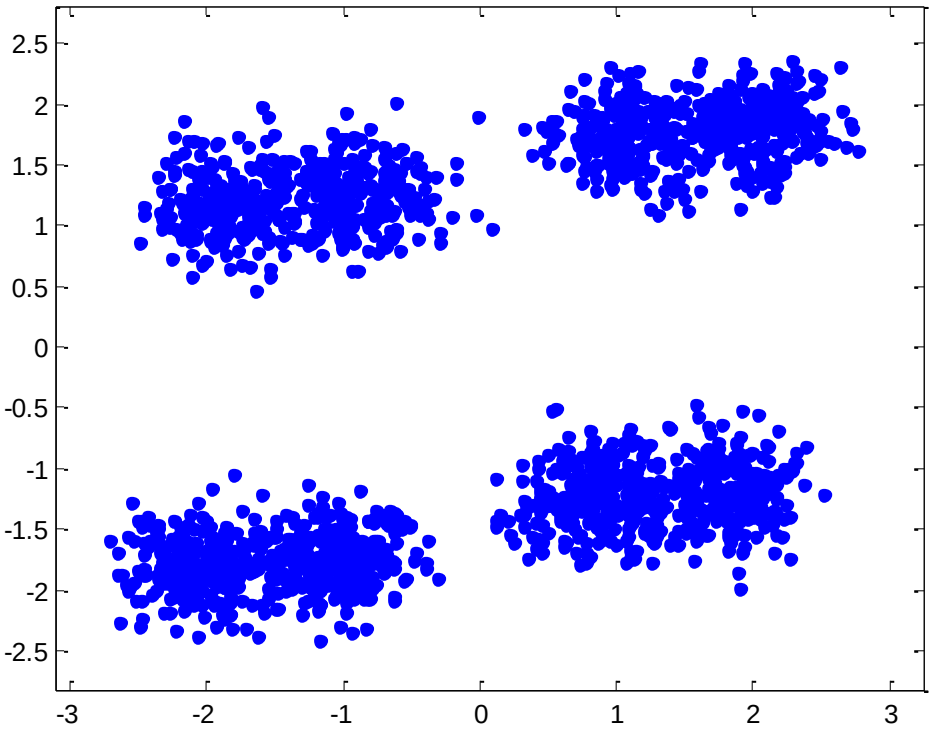

Figure 5.24 Constellation of the received signal with rough pre-equalization.

7. The Fine Post-equalization with Rough Pre-equalization

This simulation employs both fine post-equalization and rough pre-equalization. They work together at the transmitter and the receiver.

The transmitted signal and the equalized signal are plotted in Figure 5.25.

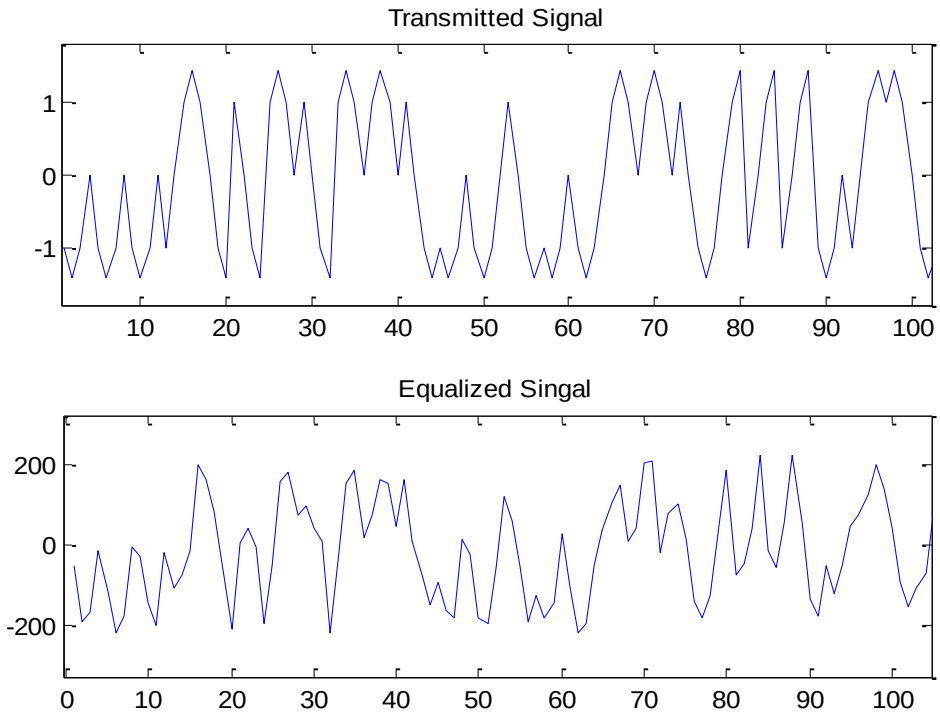

Figure 5.25 Transmitted and equalized signals.

The transmitted spectrum, pre-equalized spectrum, and post-equalized spectrum are compared in Figure 5.26.

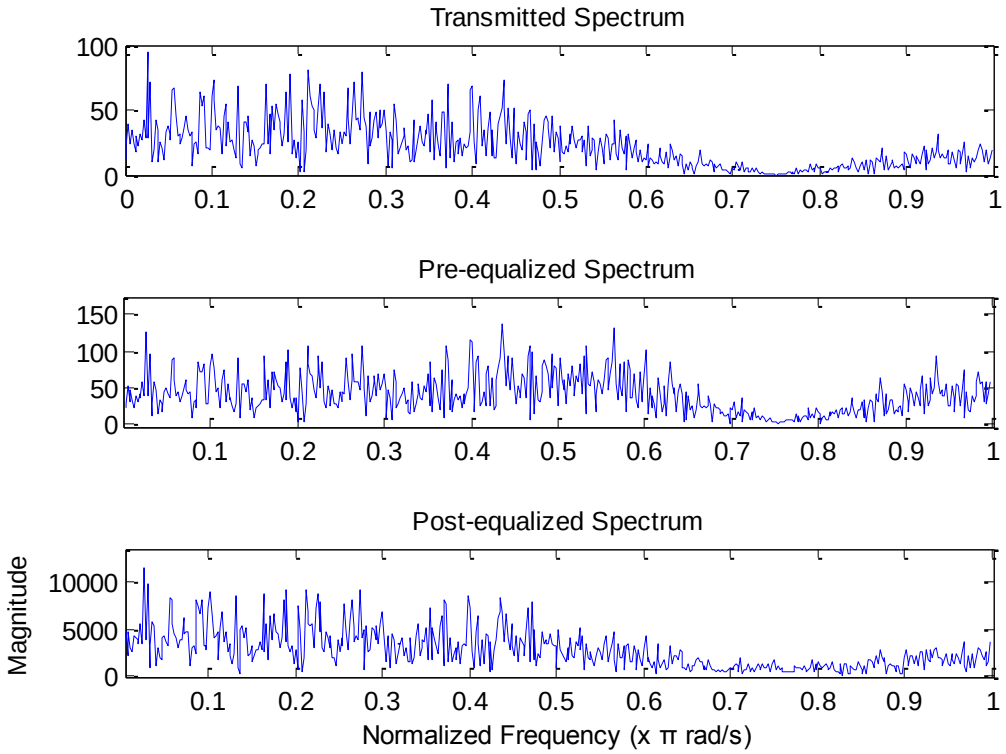

Figure 5.26 Spectrum comparison.

The constellation of the equalized signal is plotted in the Figure 5.27.

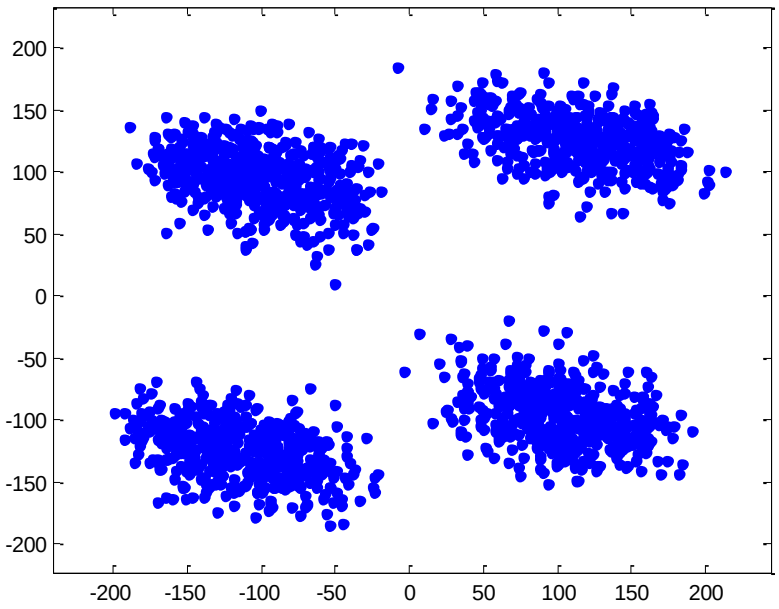

Figure 5.27 Constellation of the equalized signal.

8. Symbol Error Rate (SER) Comparison

In Figure 5.28, symbol error rate (SER) performances are compared among different equalization methods and non-equalized detection. It shows that when using equalization, much lower error rates occur for the same SNR.

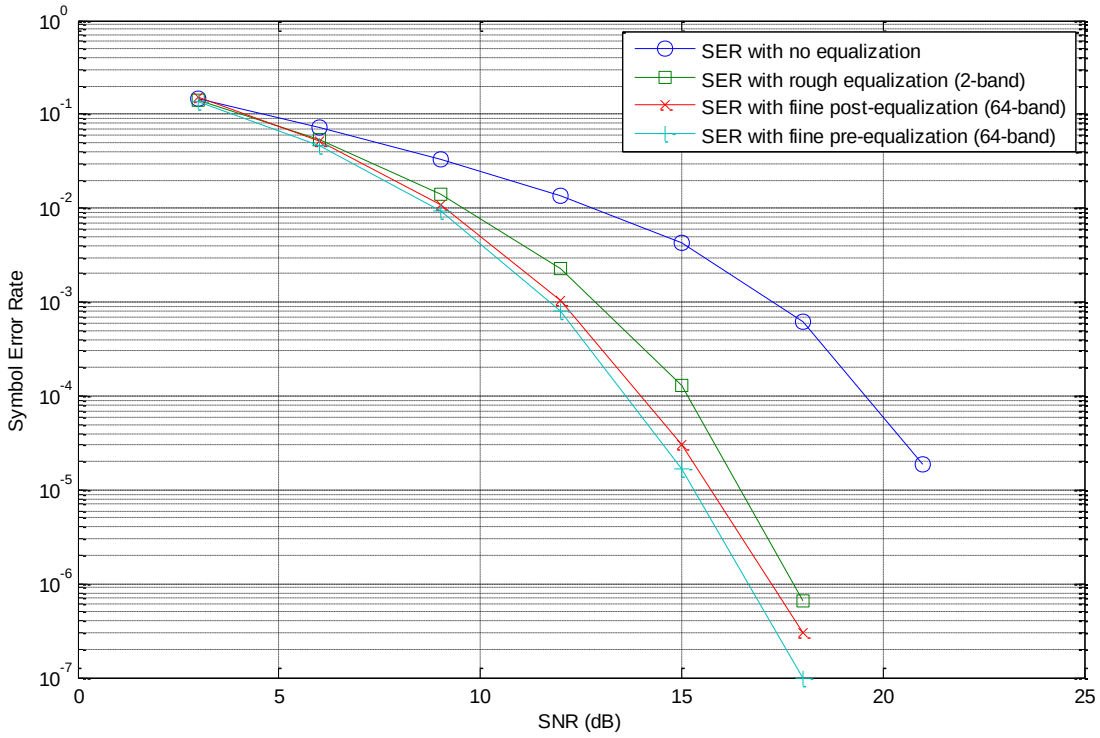

Figure 5.28 Symbol Error Rate (SER) Comparison.

5.5 PAPR Comparison

In Figure 5.29, the peak-to-average power ratios (PAPR) of three different schemes are compared. X-axis represents a given PAPR value (PAPR0) in dB, and Y-axis represents the probability that the actual PAPR is less than or equal to the given PAPR0. The result shows OFDM has the highest PAPR, which is about 8dB greater than a single-carrier QPSK. Pre-equalized QPSK signal has a little higher PAPR than regular QPSK (about 3dB).

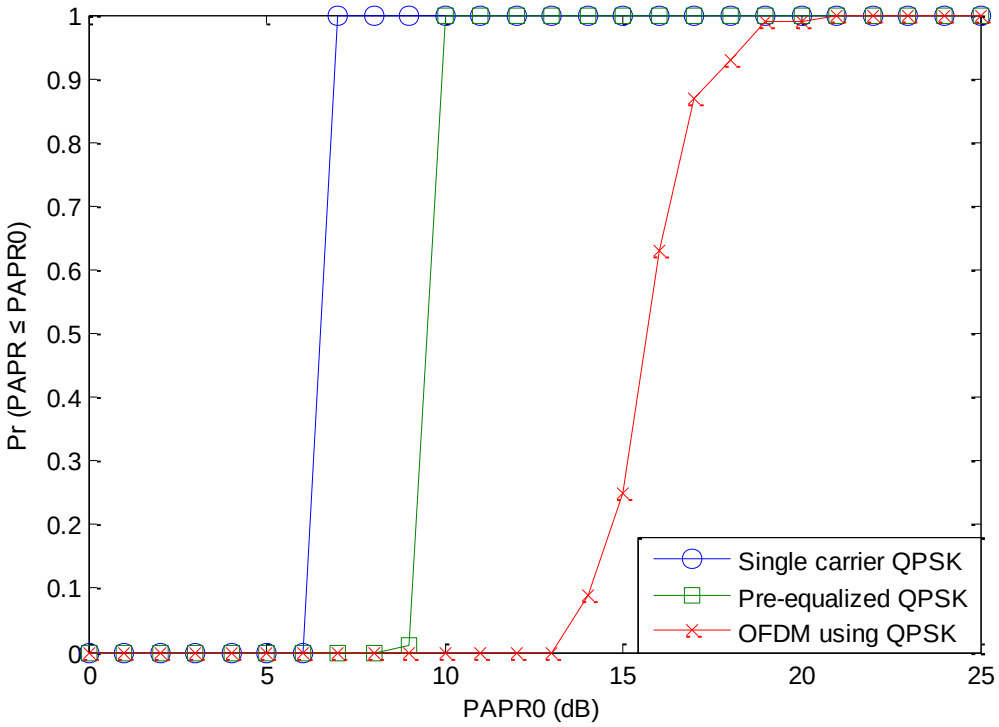

Figure 5.29 PAPR comparison among Post-equalization SCFDE, Pre-equalized SCFDE, and OFDM (all using QPSK).

CHAPTER 6

CONCLUSIONS

From the discussions and simulations in the previous chapters, the following ideas are shown and proved.

SCFDE is an effective method to combat ISI and frequency selective fading. Symbol error rate is effectively reduced by employing frequency domain equalizers.

Subband decomposition is a flexible technique to be employed to SCFDE, providing adjustable frequency resolution of equalization.

As a single-carrier transmission scheme, SCFDE provides much lower PAPR than multi-carrier transmissions, which is an advantage in optical wireless communications.

Combining with the non-negative transmission method, the SCFDE scheme with subband equalization is a good choice for high-rate optical wireless communications.

REFERENCES

[1] K. Acolatse, Y. Bar-Ness, and S. KateWilson, "Novel Techniques of Single-Carrier Frequency-Domain Equalization for Optical Wireless Communications," EURASIP Journal on Advances in Signal Processing, vol. 2011

[2] K. Acolatse, Y. Bar-Ness, Sarah Kate Wilson, "SCFDE with Space-Time Coding for IM/DD Optical Wireless Communication," Wireless Communications and Networking Conference (WCNC), pp.1694-1699, 28-31 March 2011

[3] T. Buzid, S. Reinhardt, M. Huemer, "SC/FDE, OFDM and CDMA: A Simplified Approach," Proceedings of the 9th European Conference on Wireless Technology, pp.170-173, 10-12 Sept. 2006

[4] J. Coon, J. Siew, M. Beach, A. Nix, S. Armour, and J. McGeehan, "A Comparison of MIMO-OFDM and MIMO-SCFDE in WLAN Environments," Global Telecommunications Conference, pp. 3296- 3301 vol.6, 1-5 Dec. 2003

[5] M.P. Wylie-Green, "A Power Efficient Continuous Phase Modulation - Single Carrier FDMA Transmission Scheme," Wireless Telecommunications Symposium, pp.267-272, 24-26 April 2008

[6] H.G. Myung, Lim Junsung, D.J. Goodman, "Peak-to-Average Power Ratio of Single Carrier FDMA Signals With Pulse Shaping," Personal, Indoor and Mobile Radio Communications, IEEE 17th International Symposium pp.1-5, 11-14 Sept. 2006

[7] S. Hussain, Y. Louet, "PAPR reduction of Software Radio signals using PRC method," Sarnoff Symposium 2009, IEEE, pp.1-6, March 30-April 1 2009

[8] Y. Bar-Ness, “Equalization / Intersymbol Interference,” ECE 742 Lecture Notes, NJIT, 2011

[9] Y. Bar-Ness, “Characterization of Mobile Radio Channels,” ECE 757 Lecture Notes, NJIT, 2011

[10] Choi Lai-U, R.D. Murch, “A transmit MIMO scheme with frequency domain pre-equalization for wireless frequency selective channels,” Wireless Communications, IEEE Transactions, vol.3, no.3, pp. 929- 938, May 2004

[11] Zhu Yu, K.B. Letaief, “Frequency domain pre-equalization with transmit precoding for MIMO broadcast wireless channels,” Selected Areas in Communications, IEEE Journal, vol.26, no.2, pp.389-400, February 2008

[12] I. Daubechies, “Orthonormal Bases of Compactly Supported Wavelets,” Communications on Pure and Applied Mathematics, Vol. 41, Issue 7, pp. 909–996, October 1988

[13] A.N. Akansu, R.A. Haddad, “Multiresolution Signal Decomposition: Transforms, Subbands, and Wavelets (Second Edition)”, Academic Press, San Diego, CA, 2001

[14] A.N. Akansu, “An Efficient QMF-Wavelet Structure,” Proc. 1st NJIT Symposium on Wavelets, April 1990

[15] A.N. Akansu, R.A. Haddad, H. Caglar, “The Binomial QMF-Wavelet Transform for Multiresolution Signal Decomposition,” IEEE Trans. Signal Processing, pp. 13-19, Jan. 1993

[16] A. Baskurt, H. Benoit-Cattin, C. Odet, “On the influence of the phase of conjugate quadrature filters in subband image coding,” Image Processing, IEEE Transactions, vol.7, no.6, pp. 883-888, Jun 1998

[17] Sang Wook Sohn, Hun Choi, Hyeon Deok Bae, “A subband adaptive blind equalization for MIMO system,” Circuits and Systems, MWSCAS, 51st Midwest Symposium, pp.273-276, 10-13 Aug. 2008

[18] S. Weiss, D. Garcia-Alis, R.W. Stewart, “A subband adaptive equalization structure,” Novel DSP Algorithms and Architectures for Radio Systems, IEE Colloquium, pp.4/1-4/7, 1999

[19] Damián Marelli, Minyue Fu, “A subband approach to channel estimation and equalization for DMT and OFDM systems,” Communications, IEEE Transactions, vol.53, no.5, pp.906, May 2005

[20] V.V. Vityazev, A.Y. Linovich, “A Subband Equalizer with the Flexible Structure of the Analysis / Synthesis Subsystem,” Computational Technologies in Electrical and Electronics Engineering (SIBIRCON), 2010 IEEE Region 8 International Conference, pp.174-178, 11-15 July 2010

[21] D. Marelli, Fu Minyue, “Subband Methods for OFDM Equalization,” Communications, ICC '03, IEEE International Conference, pp. 2350-2354 vol.4, 11-15 May 2003